https://doi.org/10.5194/egusphere-2024-2470
Preprint. Discussion started: 12 August 2024

Diatom shifts and limnological changes in a Siberian boreal lake: impacts of climate warming and anthropogenic pollution

Amelie Stieg[1,2], Boris K. Biskaborn[1], Ulrike Herzschuh[1,2,3], Andreas Marent[1], Jens Strauss[1], Dorothee Wilhelms–Dick[4], Luidmila A. Pestryakova[5], Hanno Meyer[1]

[1]Alfred Wegener Institute Helmholtz Centre for Polar and Marine Research, Potsdam, 14473, Germany.
[2]Institute of Environmental Science and Geography, University of Potsdam, Potsdam, 14476, Germany.
[3]Institute of Biochemistry and Biology, University of Potsdam, Potsdam, 14476, Germany.
[4]Alfred Wegener Institute Helmholtz Centre for Polar and Marine Research, Bremerhaven, 27568, Germany.
[5]Institute of Natural Sciences, North-Eastern Federal University of Yakutsk, Yakutsk, 677007, Russia.

Correspondence to: Amelie Stieg (*amelie.stieg@awi.de*), Hanno Meyer (hanno.meyer@awi.de)

https://doi.org/10.5194/egusphere-2024-2470
Preprint. Discussion started: 12 August 2024

Abstract. Lake ecosystems are affected globally by climate warming and anthropogenic influences. However, impacts on boreal lake ecosystems in Siberia, remain largely underexplored. Our aim is to determine if shifts in diatom assemblages in a remote lake in eastern Siberia are related to climate warming, similar to observations in temperate regions, while also exploring how the ecosystem might be influenced by climate and pollution through various biogeochemical proxies. We analysed continuous sediment samples from a ^{210}Pb–^{137}Cs–dated short core from Lake Khamra (59.99° N, 112.98° E), covering 220 years (ca. 1790–2015 CE), with the specific feature of combining a variety of proxies on the same sample material to provide a comprehensive record of environmental changes in this less–examined region. Biogeochemical proxies include carbon and nitrogen concentrations (TOC, TN) and corresponding stable isotopes of bulk sediment samples (δ^{13}C, δ^{15}N), as well as diatom silicon isotopes ($\delta^{30}Si_{diatom}$), alongside light microscope diatom species analysis. The diatom assemblage at Lake Khamra is dominated by few planktonic species, primarily *Aulacoseira*. At 1970 CE, we observe a significant shift in diatom assemblages, with a marked increase in the planktonic species *D. stelligera* and a decrease in *Aulacoseira*, which we attribute to recent global warming, earlier ice–out, and potential enhanced summer thermal stratification, aligning with similar changes seen in temperate lake ecosystems. Furthermore, we see evidence for an increased diatom productivity supported by rising diatom valve concentrations and accumulation rates. Carbon and nitrogen levels increase in the 1950s, preceding the 1970 CE shift in diatom assemblages, suggesting that hydroclimatic and fire–related changes in the catchment significantly influence the limnology. Increased precipitation and weathering are discussed to alter silica sources leading to decreasing $\delta^{30}Si_{diatom}$ after 1970 CE and suggest $\delta^{30}Si_{diatom}$ as a proxy for weathering rather than productivity at Lake Khamra. Indications of human impact on the lake ecosystem include a ^{13}C–depletion, linked to fossil fuel combustion since the 1950s, and changes in diatom species composition, such as the increased abundance of planktonic *A. formosa*. Furthermore, we observe a clear acidification trend since the 1990s, marked by a drastic increase in *Mallomonas* scales. Strong correlation to mercury accumulation rates, determined in a previous study, indicates a long–distance air pollution trend. We conclude the ecosystem of Lake Khamra is profoundly affected by climate warming and human–induced pollution, emphasising the urgent need for comprehensive research to address and mitigate these impacts on remote lake ecosystems to secure natural water resources.

https://doi.org/10.5194/egusphere-2024-2470
Preprint. Discussion started: 12 August 2024

1 Introduction

Human activities, particularly the burning of fossil fuels, have contributed significantly to the 'Great Acceleration' of Earth System changes especially since the 1950s (Steffen et al., 2015). Since then, the incidence of major ecological shifts in lake ecosystems globally has increased, driven by both climate change and anthropogenic impacts (Huang et al., 2022). These lake observations align with the proposed onset of the 'Anthropocene', a geological epoch beginning in the mid–20th century, introduced by Crutzen and Stoermer (2000) and further supported by Zalasiewicz et al. (2017).

Extensive research on lakes in North America and Europe (Smol et al., 2005; Smol and Douglas, 2007; Rühland et al., 2008; Kahlert et al., 2020) has shown that climate warming and human activities lead to significant ecological changes on remote high latitude ecosystems. A circumpolar study revealed major changes in the biological communities in remote Arctic lakes related to climate warming, starting as early as in the 1850s (Smol et al., 2005). However, there is a notable gap in understanding how these global changes impacted remote and less studied regions like Siberia.

Yakutia, located in eastern Siberia (Fig. 1a), experiences rapid climate warming, with annual air temperature trends showing an increase of 0.3 to 0.6°C per decade since 1966 (Gorokhov and Fedorov, 2018). Most meteorological stations report the highest temperature increases in winter, along with a rise in overall precipitation rates over the last 50 years (Gorokhov and Fedorov, 2018). Furthermore, climate warming is associated with an increase in wildfire activity (AMAP, 2021), also observed in Yakutia, which is partly due to anthropogenic alteration on the ecosystems (Kirillina et al., 2020).

There are evidences that recent warming and human–induced pollution have limnological effects in Siberia. For example, Lake Baikal, the deepest lake on Earth, showed a reduced lake ice cover duration and stronger thermal stratification since the 1950s (Roberts et al., 2018) and remote lakes in Siberia without direct human influence are also affected by the aftermath of industrialisation (Biskaborn et al., 2021b) as indicated by mercury contamination of the lake sediments and a lake acidification trend.

Diatoms, microscopic unicellular algae prevalent in nearly all aquatic environments, are effective indicators of various environmental disturbances such as climate change, acidification, and nutrient enrichment (Smol and Stoermer, 2010). They can even be linked to wildfire activity (Rühland et al., 2000). Their remains, called frustules, are composed of biogenic silica ($SiO_2 * nH_2O$), which are highly resistant and well–preserved in lake sediments. Diatom valves are suitable for light microscopic identification up to the highest species level (Battarbee et al., 2001), as well as for oxygen and silicon isotope measurements to reconstruct past climate and environmental conditions (Leng and Barker, 2006).

Circum–Arctic studies reveal climate warming, resulting in a shortened duration of lake ice covers and an extended growing season, along with thermal stratification of lake water, is the primary cause of the observed shift in diatom assemblages (Sorvari et al., 2002; Rühland et al., 2003; Rühland and Smol, 2005; Smol et al., 2005; Rühland et al., 2008; Rühland et al., 2015). However, Siberian lakes are underrepresented in circumpolar studies on diatom assemblage changes (Smol et al., 2005; Rühland et al., 2008).

In Siberia, studies analysing paleolimnological conditions through diatom assemblages, combined with diatom isotopy or biogeochemical proxies such as organic carbon, nitrogen, and mercury, are available. However, these studies predominantly cover periods within the Quaternary, primarily focusing on the Holocene and investigate long–term trends (e.g. Cherapanova et al., 2006; Biskaborn et al., 2012; Pestryakova et al., 2012; Biskaborn et al., 2016; Biskaborn et al., 2021c; Firsova et al., 2021; Kostrova et al., 2021; Mackay et al., 2022; Biskaborn et al.,

https://doi.org/10.5194/egusphere-2024-2470
Preprint. Discussion started: 12 August 2024

2023). Studies focussing on shorter time periods with a higher resolution are rare in Yakutia. Beside one study in the remote boreal areas of Siberia (Biskaborn et al., 2021b), notable study sites are located further south at Lake Baikal (Roberts et al., 2018), on Kamchatka (Jones et al., 2015), further north towards Europe (Palagushkina et al., 2020), or in the northern Urals (Solovieva et al., 2008). Hence, even if there are paleoecological studies that refer to shorter time periods, the lakes investigated are either not located in Siberia, lie in the Arctic region, or are very far south influenced by different climate regimes, as for example in North China (Yan et al., 2018).

In a previous study at the boreal Lake Khamra in southwest Yakutia, a diatom oxygen isotope record ($\delta^{18}O_{diatom}$) was established to reconstruct hydroclimatic anomalies and suggested increasing (winter) precipitation along with rising air temperatures since the 1970s (Stieg et al., 2024b). Beside oxygen isotopes, silicon isotopes of diatoms are used as paleoenvironmental proxy, for example in a lake sediment record form South China (Chen et al., 2012). However, studies that analyse both oxygen and silicon isotopes of diatoms from the same samples are rather rare. One example from a lake in northern Siberia focuses on the time period since the Last Glacial Maximum (Swann et al., 2010).

In this study, we test whether significant shifts in the Lake Khamra diatom assemblages occur, which can be related to climate warming, consistent with observations from temperate regions in North America and Europe. We also investigate potential limnological responses to climate and anthropogenic pollution. Our research addresses this gap by examining diatom assemblages and various biogeochemical proxies (TOC, TN, $\delta^{13}C$, $\delta^{15}N$, $\delta^{30}Si_{diatom}$) at decadal resolution since circa 1790 CE. We analyse continuous sediment samples from a short core of Lake Khamra, eastern Siberia, to provide a detailed account of environmental changes. Our specific objectives are to (I) identify historical lake ecosystem changes within a continuous diatom assemblage record, (II) evaluate lake bioproductivity and erosional input linked to climatic variations through biogeochemical proxies, and (III) assess the impact of human–induced pollution on diatom assemblages as well as the lake ecosystem.

https://doi.org/10.5194/egusphere-2024-2470
Preprint. Discussion started: 12 August 2024

2 Materials and Methods

2.1 Study site

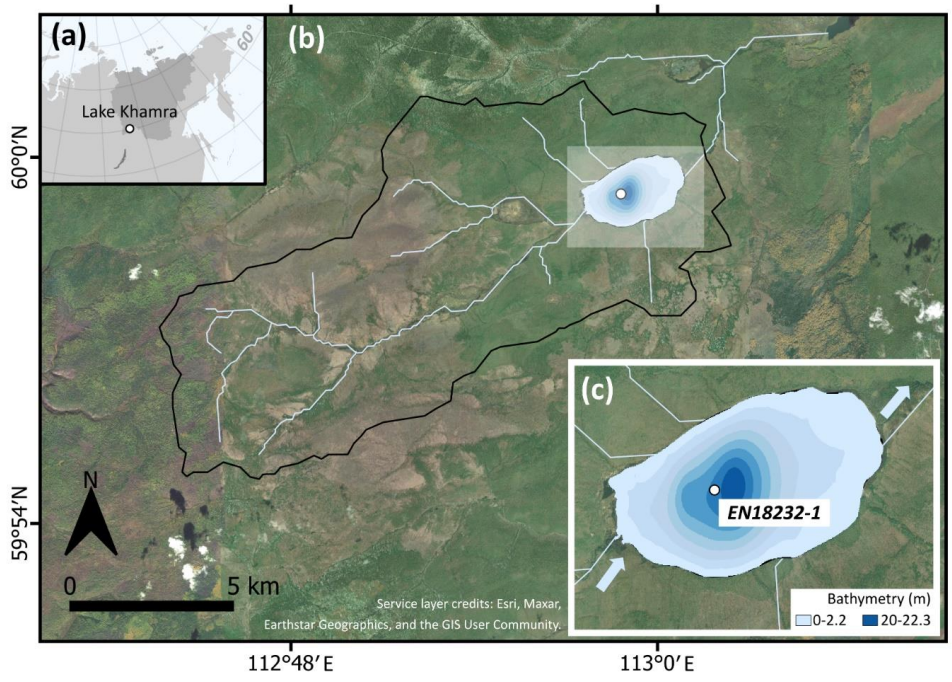

Figure 1. (a) Location of Lake Khamra in eastern Siberia, with Yakutia highlighted in darker grey. (b) Catchment of Lake Khamra. (c) Bathymetry of Lake Khamra, main inflow in the SW, main outflow in the NE and drilling position of sediment core EN18232-1 in the central part of the lake. Service layer credits: Esri, Maxar, Earthstar Geographics, and the GIS User Community.

Lake Khamra (59.99° N, 112.98° E, 340 m a.s.l.) is located distant from direct human impact in the south–west of the Republic of Sakha (Yakutia), eastern Siberia, Russia, with the closest urban settlements, Peleduy and Vitim, situated 40 and 60 km to the south–west, respectively. The landscape is located in the transition zone of evergreen to deciduous needle leaf boreal forest within the ecoregion of the middle taiga (in Geng et al. (2022) after Stone and Schlesinger, 2004). According to field observations (Kruse et al., 2019; Miesner et al., 2022), the research area is covered by a mixed–coniferous forest. The annual mean ground temperature lies between 0.0–1.0 °C at a depth of 10–20 m (Shestakova et al., 2021), indicating that the study site is within a discontinuous to sporadic permafrost zone (Obu et al., 2019). Geologically, the region is underlain by Cambrian bedrock composed of alternating dolomite and limestone, interspersed with silty Ordovician sandstone and patches of clayey Silurian limestone (Chelnokova et al., 1988).

The lake morphology is characterised by shallow shore areas and a nearly central deep part with a maximum water depth of 22.3 m (Fig. 1c). The lake has a surface area of 4.6 km² and a catchment size of 107.3 km². Lake Khamra is a hydrologically open system with a main inflow in the south–west and an outflow in the north–east and an estimated average long–term discharge of 1.1 $m^3 s^{-1}$ (Messager et al., 2016). In winter, the lake is covered by ice and snow, observed with an average ice thickness of 0.5 m and an about 1 m thick snow cover in March 2020

https://doi.org/10.5194/egusphere-2024-2470
Preprint. Discussion started: 12 August 2024

(Biskaborn et al., 2021a). Temperatures measured in the water column during that time ranged from 2 to 2.7 °C. A surface water sample taken during a summer field campaign in 2018 revealed a pH value of 6.07 and a conductivity of 40 µS/cm (Stieg et al., 2024b).

The nearest weather station is located in the town of Vitim (59.45° N, 112.58° E; 186 m a.s.l.; ECA (European Climate Assessment) station code 3235). Details and a climate diagram for the study site can be found in Stieg et al. (2024b). In relation to this, the regional climate is continental, expressed in extremely cold and dry winters (January: -28.8°C mean temp., 1929–2018 CE) and warm and humid summers (July: +18.1°C mean temp., 1929–2018 CE). The annual precipitation average at Vitim reaches 423 mm (1929–2018 CE), while the mean annual air temperature is at -5.0 °C.

2.2 Fieldwork, subsampling and core dating

Coring activities at Lake Khamra were conducted during a summer expedition in 2018 (Kruse et al., 2019). The sediment short core EN18232-1 was obtained with an UWITEC Gravity corer (60 mm) from the central and deepest part of Lake Khamra (59.99091°N, 112.98373°E; 22.3 m), based on water–depth measurements determined with a surveying rope and a portable HONDEX PS-7 LCD digital sounder. The sediment core with a total length of 42 cm was transported in a PVC tube to the Alfred Wegener Institute (AWI) in Potsdam, where it was stored dark and cool at 4°C until further analysis. The sediment core was subsampled in 1 cm continuous increments (n=39) in October 2021. The rim material (<0.5 cm) was removed to avoid possible contamination due to mixing. Furthermore, water content and dry bulk densities were determined (Stieg et al., 2024b). All subsamples were freeze–dried for at least 48 h before further processing.

We use the age–depth model for the short core EN18232-1 published by Stieg et al. (2024b), providing a comprehensive 220–year record (ca. 2015–1790 CE, mean ages) with a sub–decadal resolution according to mean ages (5.7 ± 1.7 years). The chronology relies on analysis for ^{210}Pb, ^{226}Ra, ^{137}Cs, and ^{241}Am using direct gamma assay techniques with Ortec HPGe GWL series well–type coaxial low background intrinsic germanium detectors, conducted at the Liverpool University Environmental Radioactivity Laboratory as described by Appleby et al. (1986). The age–depth model of the short core was calculated with a Bayesian accumulation model within the R package ‘rbacon’ v2.5.8 (Blaauw and Christen (2011); R version 4.1.1), based on the ^{210}Pb chronology, shown in Fig. A1 in the appendix. In addition, data on the water content and the average dry bulk density of the short core were determined, with the latter being used to calculate sedimentation rates (SR, cm a^{-1}) and mass accumulation rates (MAR, g cm^{-2} a^{-1}) downcore (Stieg et al., 2024a).

2.3 Biogeochemical proxies

The total organic carbon (TOC) and total nitrogen (TN) of 39 samples were determined to analyse historical changes of the organic matter content in the lake sediments. Freeze–dried subsamples were ground to obtain a homogeneous material. TOC was analysed by using an Elementar soli TOC cube. Total carbon (TC) was computed by the sum of TOC and the total inorganic carbon (TIC), published in a previous study (Stieg et al., 2024b). Organic carbon accumulation rates (OCARs, g m^{-2} a^{-1}) were derived by dividing TOC by 100, multiplying it by the mass accumulation rates (MAR) * 10,000 to g m^{-2} a^{-1} unit. TN was quantified by an Elementar rapid MAX N exceed. The measurement accuracy was 0.1 % for both devices, carried out at the BioGeoChemistry Lab at AWI Potsdam.

https://doi.org/10.5194/egusphere-2024-2470
Preprint. Discussion started: 12 August 2024

The TOC/TN atomic ratio (C/N), as an indicator of the organic matter source, was calculated by multiplying its mass ratio by 1.167, which is the ratio of the atomic weights of nitrogen and carbon (Meyers and Teranes, 2001). The stable carbon isotope ratio ($^{13}C/^{12}C$) of all freeze–dried and milled samples was examined, to gain additional information on past productivity and organic matter sources. Prior to isotope measurement, inorganic carbon was removed by a hydrochloric acid treatment (HCl, 1.3 mol L^{-1}). Carbon isotopes were measured by a ThermoFisher Scientific Delta-V-Advantage gas-mass spectrometer equipped with a FLASH elemental analyser EA 2000, a CONFLO IV gas-mixing system and a MA200R autosampler at the ISOLAB of AWI Potsdam. Isotope ratios are given relative to laboratory standards of known isotopic compositions and relative to the Vienna Pee Dee Belemnite (VPDB) reference standard. Nitrogen isotope ratios ($^{15}N/^{14}N$) of the 39 samples were analysed using the same gas-mass spectrometer and expressed relative to the standard atmospheric nitrogen ratio (air). Both isotope ratios are given as delta notation ($\delta^{13}C$, $\delta^{15}N$) in per mill (‰), with 1σ standard errors better than ± 0.15 ‰.

2.4 Diatom purification process and silicon isotopes

In a previous study (Stieg et al., 2024b), which focused on the oxygen isotopes of diatoms of the sediment short core EN18232-1, a comprehensive description of the diatom isotope purification procedure of the samples is provided. The silicon isotope composition was determined from the same aliquots (Leng and Sloane, 2008). In general, the purification assessment of diatom samples includes wet chemical as well as physical preparation steps (Morley et al., 2004; Leng and Barker, 2006). Essentially, the cleaning procedure included the removal of organic matter with H_2O_2 (30 %), eliminating carbonates by using HCl (10 %) and multiple heavy liquid separations (HLS) with sodium polytungstate solutions (SPT) with decreasing densities (EN18232-1: 2.50–2.12 g cm^{-3}) to separate the diatom valves from the heavy minerogenic fraction. High purity of the diatom samples was supported by a contamination assessment using a JEOL M-IT500HR analytical scanning electron microscope (SEM) with an integrated Energy–Dispersive X–ray Spectroscopy (EDS) system.

The laser fluorination method was applied using bromine pentafluoride (BrF_5) as a reagent to completely extract oxygen from the diatom SiO_2 (Clayton and Mayeda, 1963), after employing the inert Gas Flow Dehydration method (Chapligin et al., 2010). The released silicon component combines thereby with BrF_5 to silicon tetrafluoride (SiF_4). The separation of SiF_4 from the bromine compounds was achieved using a cold trap, composed of a slush of ethanol cooled with liquid nitrogen (N_2) at -115 °C. SiF_4 was then transferred and trapped into Pyrex glass tubes for the subsequent silicon isotope analysis (Chapligin et al., 2010; Maier et al., 2013). For all samples (n=39) two SiF_4 extractions were performed (except two samples with only one extraction). The samples were measured 10 times on a MAT 252 IRMS at AWI Bremerhaven against a reference gas with known isotopic composition, calibrated to the reference quartz standard NBS–28. The data was processed for outliers by performing a Dixon test with a confidence level of 80 % (Dixon, 1953). The results are expressed as delta notation $\delta^{30}Si$ (^{30}Si / ^{28}Si) in per mill (‰). The calibration was done with the internal biogenic silica standard BFC with a known $\delta^{30}Si$ of +0.13 ‰ relative to NBS–28 (Leng and Sloane, 2008). Analytical precision determined by repeated analyses of the internal standard (n=12) was better than 0.07 ‰ (1σ of $\delta^{30}Si$). A weighted mean value for each sample measurement was calculated with a standard deviation resulting from the internal or the external consistency, depending on which value is higher.

https://doi.org/10.5194/egusphere-2024-2470
Preprint. Discussion started: 12 August 2024

2.5 Diatom analysis

Diatom slides were prepared for each of the 39 samples of the short core EN18232-1 to analyse the species assemblages. The slide preparation followed the common procedure (Battarbee et al., 2001). Aliquots of 0.10 g freeze–dried sample material were treated with H_2O_2 (30 %) at 90°C for up to 8 h to remove organic matter. The reaction was stopped and carbonates were eliminated by adding HCl (10 %). After washing with purified water, 5 ml of Microsphere suspension (2 x 10^6 microspheres ml^{-1}) were added to estimate the diatom valve concentration (DVC, Battarbee and Kneen, 1982). In addition, 1 drop of ammonia (NH_3) solution was added to each sample to prevent clumping of diatom valves. The homogenised sample solution was transferred onto cover slips using Battarbee cups and mounted to slides using Naphrax. A minimum of 350 diatom valves in each sample were counted along transects (mean: 391 valves) by using a ZEISS AXIO Scope.A1 light microscope with a Plan–Apochromat 100x/ 1.4 Oil Ph3 objective at 1000x magnification. Diatom species were identified to lowest possible taxonomic level by using identification literature (Krammer and Lange-Bertalot, 1991; Krammer et al., 1991; Krammer and Lange-Bertalot, 1997b, a; Hofmann et al., 2011). Diatom nomenclature and synonyms were applied using online databases such as Diatoms.org (https://www.diatoms.org; last access: 01. August 2024; Spaulding et al., 2021) and AlgaeBase (https://www.algaebase.org; last access: 01. August 2024; Guiry and Guiry, 2024), for some species further supported with input by members of the diatom community online platform DIATOM–L (Bahls, 2015).

In addition, silicified chrysophyte *Mallomonas* scales were counted without further specification to calculate the *Mallomonas* index, which measures *Mallomonas* in relation to diatom cells (M/D) to evaluate lake acidification (Smol et al., 1984; Biskaborn et al., 2021b). The ratio of planktonic–to–benthic diatoms (P/B) of the most abundant species was calculated, excluding tychoplanktonic species, as an additional indicator of paleoenvironmental change. Habitat assignment followed mainly the online database Diatoms.org (https://www.diatoms.org; last access: 01. August 2024; Spaulding et al., 2021) and habitat information from Barinova et al. (2011). Furthermore, the abundances of the dominant *Aulacoseira* species (*Aulacoseira subarctica* and *Aulacoseira ambigua*) were summarised to better identify the assemblage changes in relation to the planktonic taxa *Discostella stelligera*.

2.6 Data processing and statistical analyses

For data processing and statistically analyses, we used the R environment (R Core Team, 2024). Diatom species richness (alpha diversity) and evenness (effective richness) were assessed by calculating Hill's N0 and N2 (Hill, 1973), with a rarefaction of the data set based on the count's minimum (n = 352), to prevent biases of varying sample sizes, utilising the R package 'vegan' (Oksanen et al., 2022). By categorising the diatom counts into dissolved and pristine valves, the *F* index was calculated to assess the diatom valve dissolution (Ryves et al., 2001 after Flower and Likhoshway, 1993). The *F* index has a total range between 0 and 1, whereby 1 equals a perfect preservation.

For further processing, the total counts of diatom species were converted to percentage data. With the R package 'rioja' (Juggins, 2022) constrained incremental sums–of–squares clustering (CONISS) was performed to define diatom zones in the record, after square–root transformation and Euclidean dissimilarity calculation of the percentage data of all involved species using the 'vegan' package (Oksanen et al., 2022), to ensure all species contribute meaningfully to the analysis, regardless of their abundance (Grimm, 1987). The diatom relative abundances and CONISS clustering are presented in a stratigraphic diagram using the function 'strat.plot' of the

https://doi.org/10.5194/egusphere-2024-2470
Preprint. Discussion started: 12 August 2024

'rioja' package (Juggins, 2022). The stratigraphy plot displays the predominant species only, which occur at least twice (≥ 2 samples) with a minimum abundance of 2 %.

The length of gradient variation of the percentage data was determined by a detrended correspondence analysis (DCA), calculated in standard deviation units (SD = 1.03), using the 'decorana' function of the R package 'vegan' (Oksanen et al., 2022). Following the thresholds discussed in Birks (2010), a principal component analysis (PCA) was conducted on the most abundant species (≥ 2 % in ≥ 2 samples) after square–root transformation. Additionally, data of diatom isotopes and biogeochemical proxies of the same sediment samples ($\delta^{18}O_{diatom}$, $\delta^{30}Si_{diatom}$, TOC, TN, C/N, OCAR, $\delta^{13}C$, $\delta^{15}N$, mercury, DVC, DAR, M/D) were projected onto the PCA ordination plot of diatom data using the 'envfit' function (Oksanen et al., 2022), enabling the visualisation within the taxonomical and ecological context.

Diatom accumulation rates (DARs in 10^9 valves m^{-2} a^{-1}) were calculated by multiplying the diatom valve concentration (DVC in 10^7 valves g^{-1}) with mass accumulation rates (MAR, g cm^{-2} a^{-1}) according to Birks (2010) and multiplying it by 100. Sediment proxies and diatom indices were correlated by performing a Pearson correlation by using the 'cor.test' function in the R package 'stats' (R Core Team, 2024) and displayed as correlation matrix with the package 'corrplot' (Wei and Simko, 2021).

Correlations with p–values < 0.05 were considered significant. In addition, data were correlated separately for periods before and after 1950 CE, employing mean ages, to specifically investigate possible anthropogenic effects in the lake ecosystem.

3 Results

3.1 Biogeochemical proxies and $\delta^{30}Si_{diatom}$

The TOC and TN records are strongly intercorrelated (r 0.98, $p<0.05$; Fig. 2, A2). TOC has a mean value of 9.2 % and TN has a mean of 0.9 %. Around 1800 CE, at the lower part of the core, both proxies are above their mean. Between ca.1830–1940 CE, values decline and stay below their mean, including their minima at about 1875 CE (TOC = 7.5 %, TN = 0.7 %). At the onset of the 1950s, TOC and TN values rise above the mean again and increase nearly continuously since the 1970s, reaching both their total maxima in the uppermost sample (TOC = 12.5 %, TN = 1.2 %). The C/N ratio has a mean of 12.6 and varies by ±1.4. Until the 1950s, the C/N ratio fluctuates slightly between 12.5 and 13, including two maxima at around 1800 CE and 1895 CE. Around 1950 CE, the C/N ratio shifts to lower values of about 12. In the two uppermost samples, the ratio slightly increases again towards 12.5 (Fig. 2). The values of OCAR fluctuate slightly around the mean value of 20.5 g m^{-2} a^{-1} and only fall below it from the 1950s until a minimum of 11.5 g m^{-2} a^{-1} at around 1970 CE, before rising to the maximum value of 50.6 g m^{-2} a^{-1} in the youngest sample (Fig. 2).

$\delta^{30}Si_{diatom}$ ranges between -0.29 to +0.52 ‰, with an overall mean of +0.24 ‰. Until 1970 CE, $\delta^{30}Si_{diatom}$ values stay mainly above the mean, including the absolute maximum of +0.52 ‰ around 1900 CE. Since the 1970s, $\delta^{30}Si_{diatom}$ values steadily decline and reach the absolute minimum of -0.29 ‰ in the topmost sample (Fig. 2).

$\delta^{13}C$ values are mainly above the mean of -30.6 ‰ before 1950 CE, ranging from -31.1 ‰ at about 1800 CE to the absolute maximum of -29.5 ‰ at ca. 1900 CE (Fig. 2). Since the 1950s, $\delta^{13}C$ continuously decreases towards more depleted values, including the absolute minimum of -32.3 ‰ at about 2000 CE. The $\delta^{15}N$ record shows a

https://doi.org/10.5194/egusphere-2024-2470
Preprint. Discussion started: 12 August 2024

generally low variability and follows mainly the mean value of +2.9 ‰ and varies in total by ± 0.5 ‰, with slightly enriched values between approx. 1930 and 1970 CE (Fig. 2).

The three correlation matrices, which show Pearson correlation coefficients for the total record of the short core EN18232-1 and data from before and after 1950 CE, are displayed in the appendix (Fig. A2–A4).

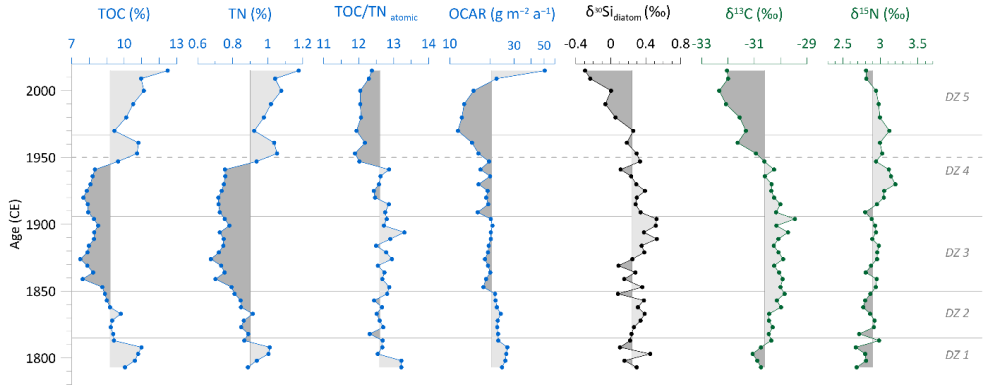

Figure 2. Biogeochemical records of the short core EN18232-1: Total organic carbon (TOC), total nitrogen (TN), TOC/TN atomic ratio (C/N), organic carbon accumulation rate (OCAR), diatom silicon isotopes ($\delta^{30}Si_{diatom}$), as well as stable carbon ($\delta^{13}C$) and nitrogen ($\delta^{15}N$) isotope values of bulk sediment samples. Vertical lines indicate the mean values. Horizontal lines indicate diatom zones (DZ), the dashed line marks the time before and after 1950 CE.

3.2 Diatom assemblages and corresponding indices

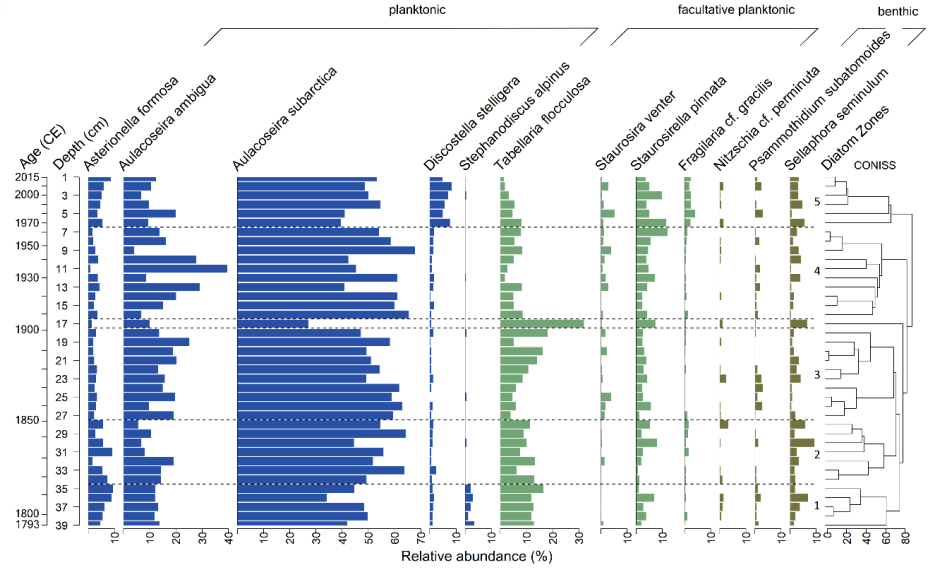

Figure 3. Relative abundances of most dominant diatom species (≥ 2 % in ≥ 2 samples) of the short core EN18232-1 versus sample depth and corresponding mean ages. Diatom zones are based on CONISS clustering shown on the right. Habitat preferences shown at the top.

https://doi.org/10.5194/egusphere-2024-2470
Preprint. Discussion started: 12 August 2024

Diatoms occur in all 39 samples of the short core EN18232-1. In total, 102 species were identified, with 12 species occurring with more than 2 % in ≥ 2 samples (Fig. 3). The valve dissolution *F* index, not displayed here, reveals overall a good valve preservation within the short core (mean: 0.84; min: 0.71; max: 0.92). The record is dominated by the planktonic cyclotelloid genus *Aulacoseira*, mainly represented by *A. subarctica* and *A. ambigua*, followed by *Tabellaria flocculosa* with a mean abundance of 8.9 %. According to the cluster analysis, we divided the diatom assemblage of EN18232-1 into five diatom zones (Fig. 3). Following percentage values refer to the mean abundance of the individual diatom species within the specific diatom zone. Only the most abundant species (n=12) are considered:

Diatom zone 1 (39–35 cm; circa 1790–1815 CE)

The first zone of the diatom record is dominated by the planktonic species *A. subarctica* (43.8 %), followed by the facultatively planktonic *T. flocculosa* (13.2 %) and the planktonic *A. ambigua* (12.7 %). Beside the two *Aulacoseira* species, the planktonic species *Asterionalla formosa* (7.0 %), *Discostella stelligera* (1.2 %) and *Stephanodiscus alpinus* (2.5 %) are also represented, at which the latter appears almost only in this diatom zone. Facultative planktonic diatom species are further represented by *Staurosirella pinnata* (3.3 %). *Fragilaria cf. gracilis* and *Staurosira venter* have low abundance with a maximum of 1 %, whereby the latter appears only once in the lowest sample. Overall benthic diatoms are the least represented, especially by *Sellaphora seminulum* (3.2 %), followed by *Psammothidium subatomoides* and *Nitzschia cf. perminuta*.

Diatom zone 2 (34–28 cm; circa 1815–1850 CE)

Diatom zone 2 is characterised by the two most abundant species *A. subarctica* (54.8 %) and *A. ambigua* (11.3 %), followed by *T. flocculosa* (10.1 %). *A. formosa* (5.4 %) show a slight decrease. Comparable to diatom zone 1, *S. pinnata* (3.2 %) represent facultative planktonic diatoms and benthic diatoms are mainly represented by *S. seminulum* (3.8 %).

Diatom zone 3 (27–17 cm; circa 1850–1910 CE)

In addition to the almost continuous dominance of *A. subarctica* (52.7 %) and *A. ambigua* (16.4 %), T. *flocculosa* shows an increase (11.4 %) and a peak around 1900 CE at the transition to zone 4 (max: 32 %), while both *Aulacoseira* taxa decline at this point. *S. pinnata* (3.5 %) and *S. seminulum* (2.2 %) also show a slight increase towards zone 4. *A. formosa* (2.6 %) continues to decline, while the facultative planktonic species *S. venter* (1.2 %) appears more frequently in this zone.

Diatom zone 4 (16–7 cm; circa 1910–1970 CE)

Dominant planktonic species are represented by *A. subarctica* (55.7 %) and *A. ambigua* (18.1 %), both reaching a maximum in this zone, while *A. formosa* (2.8 %) stays at a reduced level. Facultative planktonic diatoms are represented rather equally by *T. flocculosa* (5.9 %) and *S. pinnata* (5.1 %), the latter reaching a maximum towards zone 5 (max: 12.0 %). Benthic diatoms, *S. seminulum* and *P. subatomoides* show only minor occurrence.

Diatom zone 5 (6–1 cm; circa 1970–2015 CE)

The uppermost diatom zone is characterised by a decrease of the two dominant *Aulacoseira* species (*A. subarctica*: 47.9 %; *A. ambigua*: 11.5 %) and a clear increase of the planktonic *D. stelligera* (6.5 %) as well as of *A. formosa*

https://doi.org/10.5194/egusphere-2024-2470
Preprint. Discussion started: 12 August 2024

(5.5 %). The occurrence of *S. pinnata* (6.5 %) remains elevated and *F. cf. gracilis* (2.6 %) shows a continuous presence in this zone. The abundance of *T. flocculosa* (4.1 %) declines towards the top to its lowest values in the record. Benthic diatoms are still underrepresented mainly based on *S. seminulum* (3.4 %).

Indices, derived from the diatom data set, are presented in Fig. 4. The diatom valve concentration (DVC) increases towards the top of the core and range from 82.7 to 533.8 10^7 valves g^{-1}, with a mean of 212.2 10^7 valves g^{-1}. This results in a mean diatom valve accumulation rate (DAR) of 464.1 10^9 valves m^{-2} a^{-1} (200.98–1529.6 10^9 valves m^{-2} a^{-1}). The rarefied species richness, Hill's N0, has a mean of 21.6 and varies between 13.9 and 27.7. The evenness (effective richness), Hill's N2, result in a mean of 3.3 and span from 2.1 to 6.0. The combined abundance of *A. ambigua* and *A. subarctica*, has a mean of 66.7 % and has a similar curve to the ratio of planktonic–to–benthic diatoms (P/B). Downcore the P/B ratio fluctuate along the mean value of 24.3, before it declines to values below the mean after ca. 1950 CE. The *Mallomonas* index (M/D) has a mean of 3.5 and ranges from 0 to a clear maximum of 21.9 in the topmost sample (Fig. 4).

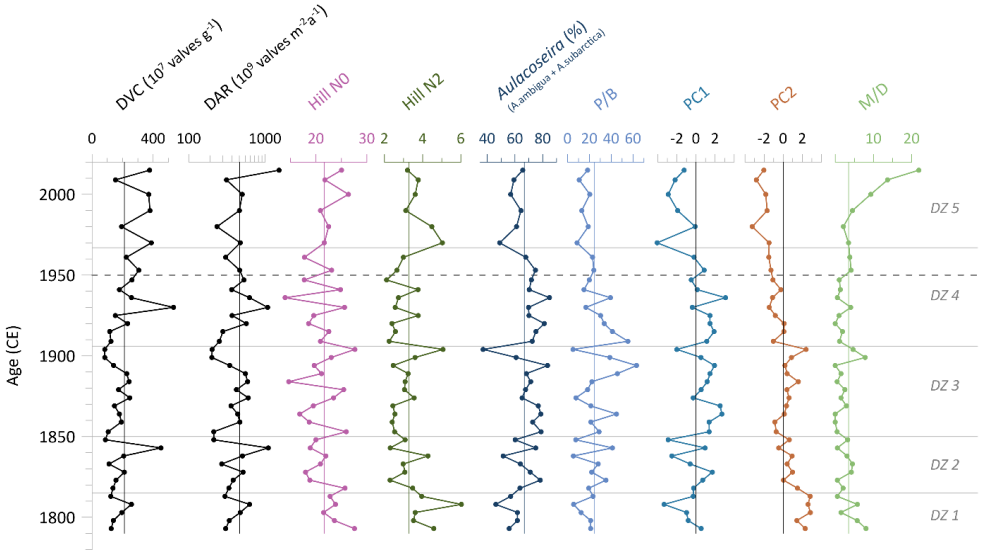

Figure 4. Statistical diatom indices of the short core EN18232-1. Diatom valve concentration (DVC), diatom accumulation rate (DAR), diatom species richness (Hill's N0) and evenness (Hill's N2), abundances of *Aulacoseira* species (*A. ambigua* and *A. subarctica*), planktonic–to–benthic species ratio (P/B) of most abundant species excluding tychoplanktonic species, main axis sample scores of principal component analysis (PC1, PC2), and the *Mallomonas* index (M/D). Vertical lines indicate the mean values. Horizontal lines indicate diatom zones (DZ), the dashed line marks the time before and after 1950 CE.

The biplot of sample scores on the first and second axes of the principal component analysis (PCA) of diatom species data explains nearly 45 % of the total variance, whereby PC1 explains 25.7 % and PC2 explains 19.2 % (Fig. 5). TOC, TN and the *Mallomonas* index (M/D) show association with the diatom species *Staurosirella pinnata* along the negative axis of PC1 and PC2 and with diatom samples after 1950 CE. Mercury, measured at the same sample material (Stieg et al., 2024b), is affiliated with the diatom species *Discostella stelligera* and *Fragilaria f. gracilis* and also points towards samples after 1950 CE. In addition, DVC and DAR point in the same direction, but are both somewhat shorter. The C/N ratio, $\delta^{30}Si_{diatom}$ and $\delta^{13}C$ display opposing clustering to the

https://doi.org/10.5194/egusphere-2024-2470
Preprint. Discussion started: 12 August 2024

previous sediment proxies along positive PC1 and PC2 axis. $\delta^{15}N$ is associated with *Staurosira venter* and *Aulacoseira subarctica* along the negative PC2 axis. OCAR is positioned along the positive PC2 axis, associated with *Tabellaria flocculosa* and *Stephanodiscus alpinus*. $\delta^{18}O_{diatom}$ does not exhibit a strong directional association with any particular diatom species.

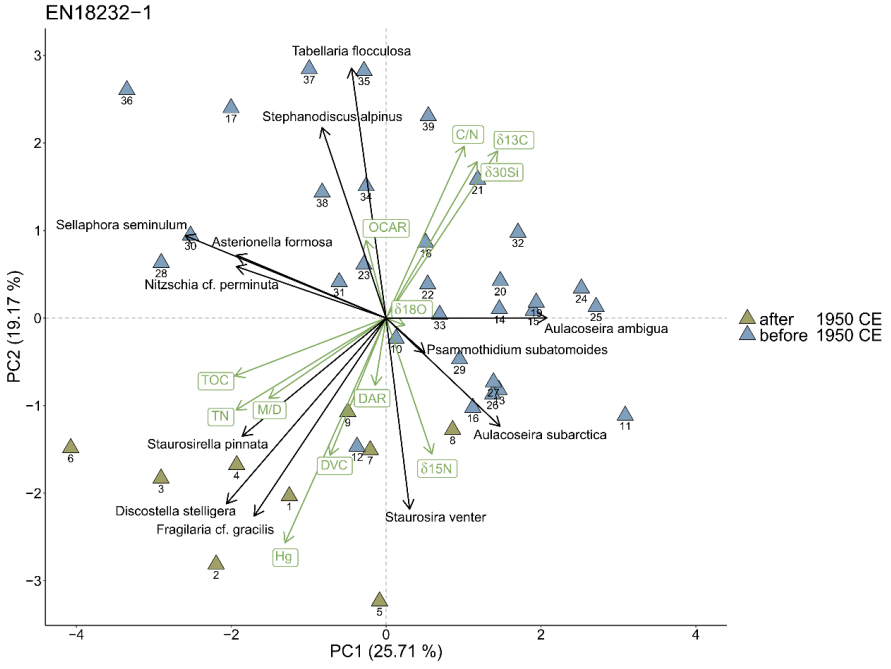

Figure 5. Biplot showing the results of the principal component analysis (PCA) with its first two dimensions (PC1, PC2) of the short core EN18232-1 derived from most abundant diatom species data (≥ 2 % in ≥ 2 samples) and corresponding environmental proxies. The percentage of explained variance for each principal component (PC) is displayed on the axis label. Coloured sample depths indicate mean ages before and after 1950 CE.

https://doi.org/10.5194/egusphere-2024-2470
Preprint. Discussion started: 12 August 2024

4 Discussion

4.1 Limnoecological interpretation of Lake Khamra diatom assemblages

Owing to the deep central part of Lake Khamra (maximum depth: 22.3 m; Fig. 1c), planktonic diatom species have been prominent over the last 220 years, as reflected by their high abundance within in the short core EN18232-1 (Fig. 3). The planktonic diatom genera *Aulacoseira*, mainly represented by *A. subarctica* and *A. ambigua*, is most abundant and common in deep, cold, unstratified lakes in the Arctic tundra (Laing and Smol, 2003). Given its large, highly silicified and thus heavy frustules which rapidly sink (Laing and Smol, 2003), *Aulacoseira* taxa rely on adequate turbulence to stay suspended within the water column (Gibson et al., 2003; Rühland et al., 2008). Thermal stratification or a perennial lake ice cover can weaken the turbulence and lead to a settlement of heavier diatom cells (Gibson et al., 2003). Temperature measurements taken under the ice in March 2020 (Biskaborn et al., 2021a) indicate very cold water temperatures (mean: 2.5 °C) and a well–mixed water column (Stieg et al., 2024b). Given that *A. subarctica* predominates throughout the record (Fig. 3), it suggests that the growth conditions at Lake Khamra generally favour this species, and a seasonal ice cover does not necessarily reduce its abundance. Furthermore, the snow–rich region and the associated inflow of cold snowmelt water (Stieg et al., 2024b) presumably lead to sufficient turbulence and nutrient upwelling in spring, which likely ensure an enduring circulation beneficial for *A. subarctica* (Horn et al., 2011).

Facultative planktonic species, mainly epiphytic (attached to plants), are less abundant and primarily characterised by *T. flocculosa* (reaching up to 32 %) and *S. pinnata* (up to 12 %; Fig. 3). Beside the deep central part, Lake Khamra has a shallow littoral area (Fig. 1c), where macrophytes are likely find favourable growing conditions that provide habitat for epiphytic diatom taxa. Purely benthic diatoms (*N. cf. perminuta*, *P. subatomoides*, *S. seminulum*) are of low abundance at Lake Khamra and reach a maximum of 3 % to 9 %. Light limitations due to the lake depth, annual ice cover and cold water temperatures as well as the availability of nutrients likely regulate the abundance of benthic taxa. The rarefied species richness (mean Hill's N0: 21.6) and evenness (mean Hill's N2: 3.3) are rather low, also suggesting a few species dominate Lake Khamra.

In general, the diatom assemblage of the short core EN18232-1 characterises a deep, open freshwater lake in the boreal forest biome with oligotrophic conditions over the last 220 years. We observe a high diatom valve concentration (DVC, mean $212*10^7$ valves g^{-1}) within the short core, compared to e.g. a surface sediment lake core from the Siberian Arctic (Biskaborn et al., 2023) or to another pristine lake in Yakutia (Biskaborn et al., 2021b). This likely indicates favourable growth conditions at Lake Khamra that enhance diatom productivity and reflect good preservation environments, as evidenced by an overall high *F* index (mean: 0.84) of the short core. These factors and the subdecadal resolution of the short core make the lake suitable for paleoecological studies.

4.2 Linking diatom assemblage shifts to hydroclimatic and lake environmental changes

4.2.1 Diatom zone 1: A reduction of main *Aulacoseira* taxa align with reduced winter precipitation

The diatom assemblage of the short core is subdivided into five diatom zones. In **diatom zone 1** (1790–1815 CE), we observe a dominance of the planktonic diatom genera *Aulacoseira*, mainly represented by the species *A. subarctica* and *A. ambigua.* However, the abundance of *Aulacoseira* is reduced compared to the following three diatom zones, similarly low as in the most recent zone after 1970 CE (Fig. 4). At the time of diatom zone 1, a hydroclimatic reconstruction from Lake Khamra, reconstructed by using a $\delta^{18}O_{diatom}$ record of the same sediment

https://doi.org/10.5194/egusphere-2024-2470
Preprint. Discussion started: 12 August 2024

samples, indicates a rather dry and cool period (1790–1830 CE) with reduced winter precipitation (Stieg et al., 2024b). It is assumed that less precipitation in winter, accumulated as snow, leads to reduced snowmelt water inflow into the lake. This could lead to reduced water turbulence in spring and hence less favourable conditions for *Aulacoseira* to bloom. In contrast, the planktonic species *A. formosa* and *S. alpinus* have thrived during diatom zone 1, whereas the latter occurs only in this zone. *S. alpinus* is reported rarely and appears in oligotrophic lakes with very low water temperatures (Häkansson and Kling, 1989; Krammer et al., 1991). The corresponding genera *Stephanodiscus* prefers high electrical conductivities and high dissolved silica concentrations (Häkansson and Kling, 1989; Pestryakova et al., 2018) and appears globally in fresh as well as slightly saline waters (Häkansson and Kling, 1989). *A. formosa* is reported to have a broad nutrient tolerance range (Rimet et al., 2009; Wang et al., 2012) but it commonly thrive in nutrient–rich lakes (Reynolds et al., 2002; Wang et al., 2012; Rühland et al., 2015). A reduced meltwater inflow due to overall relatively dry winter conditions could have led to a lower lake level at Lake Khamra, supported by a low P/B ratio (Fig. 4) (Wolin and Stone, 2010), and a proportionally higher nutrient concentration during that phase (Moos et al., 2009), likely beneficial for *S. alpinus* and *A. formosa*.

Facultative planktonic species are primarily represented by epiphytic *T. flocculosa* and *S. pinnata* in diatom zone 1 (Fig. 3). *T. flocculosa* has the second highest abundance in this diatom zone and can occur in both benthic as well as planktonic habitats (Heudre et al., 2021). It implies neutral to slightly acidic and nutrient–enriched conditions (Palagushkina et al., 2012; Biskaborn et al., 2023), aligning with an assumed higher nutrient concentration at Lake Khamra during that time. *S. pinnata*, as a synonym of *Fragilaria pinnata* (Guiry and Guiry, 2024), is a small tychoplanktonic diatom (Narancic et al., 2016) and is most common in lakes within northern forests (Pestryakova et al., 2018). A reduced input of snowmelt water and a reduced lake level could have increased littoral habitats at the shallow shore areas of Lake Khamra (Fig. 1c), accompanied by increased water plant growth in summer and, thus, also increase the habitat possibilities for these facultative diatoms. Furthermore, cold conditions might have led to an extensive and long–lasting ice cover at Lake Khamra. *S. pinnata* as a small fragilarioid taxon, demonstrates resilience to cold water temperatures and lives in the benthos during lake ice cover (Biskaborn et al., 2012). A prolonged lake ice cover could additionally weaken lake water turbulence and further explain the observed decline in *Aulacoseira* abundance, leading to a settlement of the diatom cells (Gibson et al., 2003). Elevated diatom species richness until 1815 CE (Hill's N0 and N2, Fig. 4), mirror the reduced abundance of the main *Aulacoseira* taxa and the relevance of other diatom species in diatom zone 1.

4.2.2 *Diatom zones 2 to 4: Aulacoseira* dominance linked to melt water inflow

In **diatom zone 2** (1815–1850 CE) both *Aulacoseira* species clearly increase in abundance and together reach up to about 75 % (Fig. 4), in parallel with the disappearance of *S. alpinus* and a slight reduction of *A. formosa*. The dominance of *Aulacoseira* is also reflected in a decrease in species richness indicated by declining Hill numbers (Fig. 4). *A. formosa* is considered to be a competitor of the two dominant *Aulacoseira* taxa (indicated by the opposite directions in the PCA; Fig. 5), as it prefers similar conditions such as water turbulence to avoid sinking, and enhanced stratification primarily terminates the growth of *A. formosa* (Wang et al., 2012). The hydroclimatic reconstruction suggests a shift from dry to wet at 1830 CE followed by a prolonged rather stable period with the lake water primarily influenced by snowmelt until 1930 CE (Stieg et al., 2024b). A rise in snowmelt water input presumably provide sufficient turbulence and a nutrient upwelling beneficial for *A. subarctica* (Horn et al., 2011). Moreover, a higher meltwater input potentially lowers the lake water conductivity, less favourable for

https://doi.org/10.5194/egusphere-2024-2470
Preprint. Discussion started: 12 August 2024

Stephanodiscus sp. (Pestryakova et al., 2012). Additionally, sufficient meltwater supply likely stabilised the lake at a higher water level, profitable for planktonic species, and further supported by an increase of the P/B ratio (Wolin and Stone, 2010) at the onset of diatom zone 2 (Fig. 4).

In **diatom zone 3** (1850–1910 CE) the dominance of *Aulacoseira* stabilises (Fig. 4), further displacing *A. formosa* (Fig. 3), displayed in the rather low level of effective species richness (Hill's N2, Fig. 4). *T. flocculosa* thrives in diatom zone 3 and reaches an absolute maximum (32 %) around 1900 CE, while *Aulacoseira* reaches an absolute minimum (37 %) in one sample. This shift is potentially a reaction to unstable habitat conditions of *T. flocculosa* (Palagushkina et al., 2012), such as transient hydrological changes that had short–term consequences for both planktonic and benthic diatom habitat conditions (Rühland et al., 2015; Biskaborn et al., 2023). A study of a Canadian lake indicates that some taxa, including *T. flocculosa*, show a significant increase with fire disturbance, while planktonic taxa decrease (Philibert et al., 2003). This pattern suggests a similar response in Lake Khamra, where evidence of wildfires around 1880 CE in the lake vicinity (Glückler et al., 2021), marked by a peak in charcoal (Fig. 6), likely caused a short–term disturbance in environmental conditions. Light limitations due to surface and dispersed particles, as suggested by Philibert et al. (2003), could be one possibility, leading to increased growth of *T. flocculosa* and a concurrent decrease in *Aulacoseira*. However, as this shift is based on only a single sample, it should be interpreted with caution.

S. venter establishes in diatom zone 3 and also *S. pinnata* stays at a rather constant abundance, however both remaining on a low level (Fig. 3). Both are small fragilarioid taxa, which are adapted to short growing phases and known as pioneering and opportunistic species, occurring in oligotrophic–neutral to alkaline lakes (Biskaborn et al., 2012; Pestryakova et al., 2012; Narancic et al., 2016). Their presence coincides with the dominant influence of winter precipitation on the lake water, which tends to create difficult growing conditions for epiphytic diatoms.

Diatom zone 4 (1910–1970 CE) is still characterised by a high abundance of *Aulacoseira*, but clearly decreasing from a maximum at ca. 1935 CE (ca. 85 %) to a minimum at ca.1970 CE (of ca. 50 %; Fig. 4), indicating high variability. Meteorological data from the nearest weather station in Vitim, starting in the 1930s, suggest a precipitation deficit, especially in winter precipitation, aligning with a variable hydroclimatic phase including a dry anomaly around the 1950s (Stieg et al., 2024b) and an increase in wildfire activity in the vicinity of the lake (Glückler et al., 2021; Stieg et al., 2024b). A reduction of turbulence, caused by reduced snowmelt water supply during spring bloom, seems a reasonable explanation for the decline of *Aulacoseira*. PC1 reaches a minimum associated with the decrease of *Aulacoseira* species (Fig. 4). Comparable to the transition from diatom zone 1 to 2, we simultaneously observe an increase in diatom evenness between 1950 and 1970 CE (Hill's N2, peak in the 1970s; Fig. 4), which indicates a shift towards better habitat conditions in favour of epiphytic and benthic diatoms. A reduction in precipitation likely led to a decreased lake level, thereby increasing littoral habitats and macrophyte growth in the shallow shore areas of the lake, contributing to a more complex diatom community.

Facultative planktonic diatoms remain relatively constant, except for *S. pinnata*, which shows a maximum around 1970 CE (Fig. 3), which could be a response to increased fire activity. There are reports that certain diatom species, such as *Fragilaria pinnata*, *F. construens var. venter*, and *Tabellaria quadriseptata*, become more abundant during fire intervals (Rühland et al., 2000), based on a peat core analysis in Siberia (Jasinski et al., 1998), linked to enhanced weathering and increase silt deposition (Rühland et al., 2000).

https://doi.org/10.5194/egusphere-2024-2470
Preprint. Discussion started: 12 August 2024

4.2.3 Diatom zone 5: Diatom shift at 1970 CE: A climate warming signal

We observe a significant shift in diatom assemblage at 1970 CE, separating diatom zones 4 and 5 (Fig. 3). **Diatom zone 5** (1970–2015 CE) is characterised by a significant increase in the planktonic *D. stelligera*, rising from low relative abundances up to 8.5 %, while both *Aulacoseira* species show a minimum (Fig. 6). *D. stelligera* (synonym *Cyclotella stelligera;* Guiry and Guiry, 2024), belongs to diatoms of the *Cyclotella sensu lato* taxa (Saros and Anderson, 2015). The shift in diatom assemblage characterised by an increase of small cyclotelloid planktonic diatoms like the *Cyclotella stelligera* complex and a simultaneously decrease of *Aulacoseira* taxa and/or small benthic fragilariod taxa is revealed in other paleolimnological studies on the northern hemisphere (Rühland et al., 2003; Smol et al., 2005; Rühland et al., 2008). Diatom zone 5 corresponds with a hydroclimatic phase of the $\delta^{18}O_{diatom}$ record, indicating increased winter precipitation and more snowmelt water in Lake Khamra, as supported by meteorological data (Stieg et al., 2024b). Despite increased water turbulence from inflow, which usually benefits *Aulacoseira*, its observed decrease is unexpected. Therefore, we infer that an additional factor is responsible for the decline. In the 1970s regional annual temperature start to increase (Anomalies of annual mean temperature, Vitim; Fig. 6). Rising temperatures, in the context of global warming, likely reduce the ice–cover duration and increases the possibility of thermal stratification of the lake water in the ice–free period, allowing *D. stelligera* to thrive (Smol et al., 2005; Rühland et al., 2015), less favourable for *Aulacoseira* (Gibson et al., 2003; Rühland et al., 2008), although it remains dominant at Lake Khamra (>50 %, Fig. 4).

In many Arctic lakes, comparable shifts in the diatom community occurred as early as 1850 CE (Smol et al., 2005), while the change at Lake Khamra occurred about 120 years later. The timing discrepancy regarding the onset of increase in small *Cyclotella sensu lato* species aligns precisely with studied temperate regions in North America and Europe (Rühland et al., 2008), which also show a change from 1970 CE onwards. Siberian lakes are rare in circumpolar studies (Smol et al., 2005; Rühland et al., 2008). Nevertheless, a similar shift in diatom composition has been observed at a comparable remote boreal lake in eastern Siberia after 1850 CE, as a response to climate warming (Biskaborn et al., 2021b). Furthermore, analogous observations were made at the south basin of Lake Baikal at ca. 1970 CE (Roberts et al., 2018), as well as at pristine Arctic and sub–Arctic lakes in the northern Urals with most distinct shifts after 1970 CE (Solovieva et al., 2008). Our data align with the later onset of diatom assemblage changes at lower latitudes compared to the earlier changes observed in Arctic regions, which is attributed to an earlier warming and a quicker response of Arctic ecosystems compared to lower latitudes (Smol et al., 2005; Smol and Douglas, 2007).

An increase of annual temperature and a shorter lake ice period extend the diatom growing season and change light and nutrient availability, favouring small planktonic diatoms (Rühland et al., 2015). Observed elevated diatom species richness (Hill's N0, Fig. 4) are congruent with reported increased diatom community complexity and diversity during prolonged ice–free periods in Arctic lakes (Douglas and Smol, 2010; Rühland et al., 2015). During longer ice–free periods, the shallow littoral zones of Lake Khamra would be more exposed to sunlight, accelerating water heating and potentially offering better conditions for water plants to thrive. Increased macrophyte growth likely change the nutrient availability and offer new habitat for epiphytic diatoms, like *S. pinnata* or *F. cf. gracilis* (which establish in diatom zone 5, Fig. 3). Different studies have reported a rise in pennate (tychoplanktonic) planktonic Fragilaria populations as a response to climate warming (Rühland et al., 2013; Michelutti et al., 2015; Sochuliakova et al., 2018). *S. pinnata* and *F. cf. gracilis* both plot together with *D. stelligera* in the PCA biplot (Fig. 5), underlining a possible common reaction to warming at Lake Khamra.

https://doi.org/10.5194/egusphere-2024-2470
Preprint. Discussion started: 12 August 2024

The shifts in diatom assemblage delineating zones 4 and 5 as well as 1 and 2 have similarities (*Aulacoseira* decline while planktonic cyclotelloid taxa such as *S. alpinus* or *D. stelligera* increase and diatom richness increase). However, we also see clear differences (cold habitat preferences from *S. alpinus* vs. warm and stratified preferences of *D. stelligera*, increase of *F.cf. gracilis* and *S. pinnata* in recent years only) which suggests that the increase in air temperatures in recent decades significantly influenced the lake ecosystem and its diatom assemblages, overprinting the influence of a simultaneous precipitation increase.

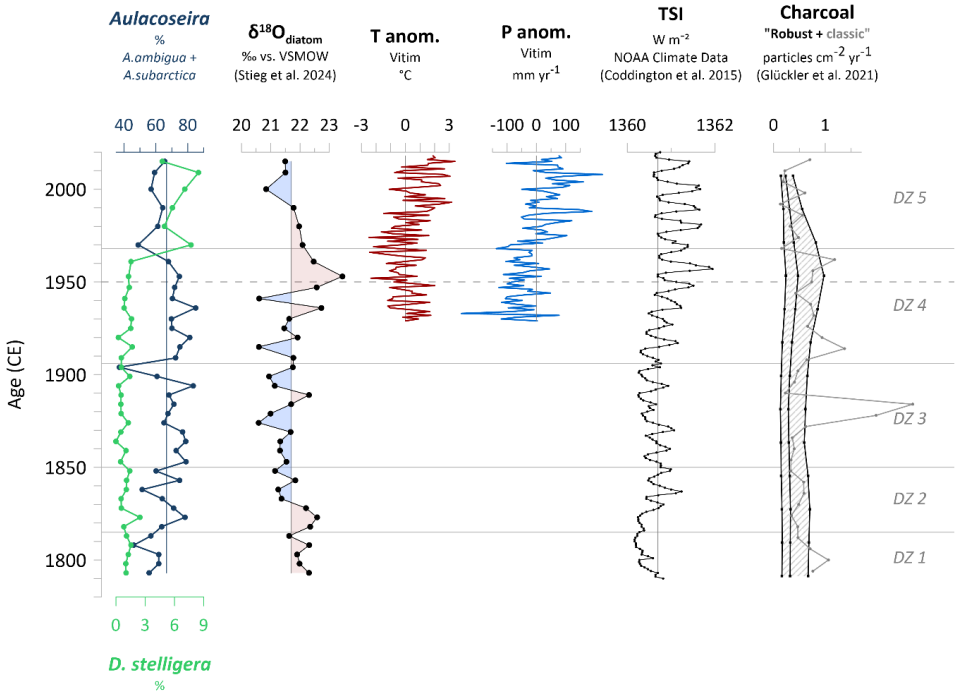

Figure 6. Comparable records as possible forcing for diatom assemblage changes: *Aulacoseira* vs. *D.stelligera* abundances of the short core EN18232-1; $\delta^{18}O_{diatom}$ record from the same short core of Lake Khamra (Stieg et al., 2024b); Anomalies of annual mean temperature and annual precipitation from the weather station in Vitim (59.45° N, 112.58° E; 186 m a.s.l.; ECA (European Climate Assessment); data accessible via the KNMI Climate Explorer https://climexp.knmi.nl; last access: 15. July 2024; Klein Tank et al., 2002); NOAA Climate Data Record of Total Solar Irradiance (TSI, Coddington et al., 2015); charcoal record from Lake Khamra, "classic" and "robust CHAR", letter accounts for accumulated uncertainties (Glückler et al., 2021). Vertical lines indicate the mean values. Horizontal lines indicate diatom zones (DZ), the dashed line marks the time before and after 1950 CE.

https://doi.org/10.5194/egusphere-2024-2470
Preprint. Discussion started: 12 August 2024

4.3 Biogeochemical proxies as indicators of bioproductivity and erosion at Lake Khamra

4.3.1 Biogeochemical shifts after 1950 CE

Carbon and nitrogen indicators (TOC, TN, C/N, OCAR, $\delta^{13}C$; Fig. 2) show a notable shift at 1950 CE, highlighting substantial limnological changes that precede the major shifts in diatom communities observed starting at 1970 CE (onset of diatom zone 5). We propose that hydroclimatic variability significantly influences limnological conditions, with some diatom species responding immediately. However, the broader shift in the diatom assemblage appears to occur later and is more likely driven by rising temperatures and their associated effects, as discussed above.

It is probable that during the dry period with less snowmelt inflow during the 1950s, as deduced by Stieg et al. (2024b), the erosional input from catchment is reduced, aligning with a low sedimentation rate during that time (also visible in the flattening of the age–depth relationship starting in the 1950s; Fig. A1). Concurrently, the accumulation rate of organic carbon (OCAR) declines to a minimum of 11.5 g m^{-2} a^{-1} from 1950 to 1970 CE (Fig. 2), aligning with the decrease of the most abundant diatom taxa *Aulacoseira* at the end of diatom zone 4. In contrast, total organic carbon (TOC) and total nitrogen (TN), which represent the fraction of organic matter and are closely related to primary productivity (Meyers and Teranes, 2001), both show a peak between 1950 and 1970 CE (Fig. 2), indicating higher bioproductivity. It is plausible, that low sedimentation rates could result in a relative increase in TOC and TN concentrations within the sediment, explaining the contrasting tendency.

We observe a similar trend in rising DVC and rather stable DAR (Fig. 4). The increase in DVC above the mean since the 1950s, indicating a shift towards enhanced diatom productivity, could potentially be linked to the increasing diatom richness (rising Hill numbers, Fig. 4) due to habitat changes as the dominant *Aulacoseira* decline. Alternatively, the higher DVC could also be attributed to low sedimentation rates, increasing its concentration. The high *F* index (mean: 0.84) supports that preservation is consistently very good across all sediment layers, indicating no significant taphonomic changes affecting the diatom signal.

During the dry period between the 1950s and 70s, the erosional input from the catchment was probably reduced. However, a differentiation between autochthonous (in–lake) or allochthonous origin of organic material since then remains indistinct. The atomic organic carbon–to–nitrogen ratio (C/N) together with $\delta^{13}C$ help to identify the organic matter origin (Meyers, 2009). C/N drops from ca. 13 to a slightly lower level of around 12 since the 1950s, reflecting a mixed signal in both cases. According to the literature, lacustrine algae have a C/N ratio ranging between 4 and 10, whereas organic matter from land plants have a ratio >20 (Meyers and Teranes, 2001). Also together with $\delta^{13}C$, a differentiation still remains inexplicit (Fig. A5), as both, algae and C_3–land plants, have similar $\delta^{13}C$ signatures, making them indistinguishable (Meyers, 2009). The $\delta^{15}N$ data underlines a mixed organic origin, as the value of 3 ‰ lies in between land plants (around 0 ‰) and freshwater algae (5–10 ‰, Meyers, 2009). However, the rather low C/N values tend towards an autochthonous organic matter source since the 1950s.

After 1970 CE, during diatom zone 5, increasing precipitation in the region (Fig. 6), suggests an increased erosional input from the catchment. Simultaneously, we observe an increase in both TOC and TN, reaching values of up to 12.5 % and 1.2 % respectively (Fig. 2), pointing towards a higher bioproductivity (Meyers and Teranes, 2001). Since OCAR increases simultaneously (Fig. 2), it supports an enhanced accumulation of TOC from 1970 CE onwards, whereby C/N still mirrors a mixed signal of its origin. The concentration of diatom valves (DVC) remains elevated past 1970 CE (Fig. 2), aligning with the appearance of *D. stelligera* in 1970 CE and the increase in (tycho)planktonic diatom taxa in diatom zone 5. The DAR lags slightly behind and increases after the 1980s,

https://doi.org/10.5194/egusphere-2024-2470
Preprint. Discussion started: 12 August 2024

indicating higher diatom productivity likely related to warming (Douglas and Smol, 2010; Biskaborn et al., 2012; Biskaborn et al., 2021b). Since diatoms are photosynthetic algae that depend on sunlight, the modern solar maximum around the 1950s and overall elevated insolation since then (Fig. 6) certainly also promoted algae growth.

The continuous decrease in $\delta^{13}C$ since the 1950s (Fig. 2) initially appears to contradict the interpretation of increased bioproductivity, even though algae and land plants have similar signatures (Meyers, 2009). In general, phytoplankton preferentially incorporates lighter ^{12}C than ^{13}C, which enriches the remaining reservoir over time and lead to increasing $\delta^{13}C$ values of organic matter during enhanced productivity (Meyers, 2009). The observed $\delta^{13}C$ decline might, at least partly, be related to fossil fuel combustion and biomass burning, which release CO_2 depleted in ^{13}C into the atmosphere, known as *Suess effect* (Keeling, 1979). As the CO_2 in the atmosphere and in the water tend to reach equilibrium, this also effects the $\delta^{13}C$ values of lake sediment organic matter (Verburg, 2007), as observed e.g. in a lake study in West Greenland (Stevenson et al., 2021). Most of the decline in $\delta^{13}C$ of about 1.7 ‰ at Lake Khamra could, thus, be explained by the decline in atmospheric $\delta^{13}C$, which has accelerated particularly after 1950 and has fallen by about 1 ‰ since then (Verburg, 2007). In a previous study, increased mercury concentrations indicated that Lake Khamra is affected by human air pollution (Stieg et al., 2024b), further confirmed by a strong correlation between $\delta^{13}C$ and mercury after 1950 CE (r -0.97, $p<0.05$, Fig. A4). Aside from that, an increased algae productivity might not contradict with decreasing $\delta^{13}C$ values, as light CO_2 can be constantly assimilated during increased growth, as observed in an Arctic lake (Jiang et al., 2011).

Like $\delta^{13}C$, $\delta^{30}Si_{diatom}$ also decreases, but slightly later at around 1970 CE (Fig. 2), which coincides with the shift of the diatom assemblages between diatom zone 4 and 5. We assume that the decrease in $\delta^{30}Si_{diatom}$ is influenced by multiple factors, as the interpretation of silicon isotopes is complex and involves various processes (Sutton et al., 2018). Overall, the $\delta^{30}Si_{diatom}$ values are low (mean: + 0.24 ‰), comparable to e.g. a study at a groundwater–dominated Swedish lake (Zahajská et al., 2021a). Groundwater inflow could lead to low isotope values of dissolved silica (DSi, $\delta^{30}Si_{DSi}$) and hence to low $\delta^{30}Si_{diatom}$ (Opfergelt et al., 2011; Frings et al., 2016; Zahajská et al., 2021b; Zahajská et al., 2021a). Unfortunately, there is no information on lake water $\delta^{30}Si_{DSi}$ or groundwater inflow at Lake Khamra. It is likely that groundwater input at Lake Khamra contributes to the generally low $\delta^{30}Si_{diatom}$. However, a sudden change in groundwater seems unlikely and cannot explain the distinct decrease at around 1970 CE.

Fractionation of silicon isotopes occurs through both inorganic chemical weathering and biological activities, mainly diatom growth in marine and terrestrial environments (Opfergelt et al., 2011). In marine environments, diatom silicon utilisation is linked with the silicon isotope composition (De la Rocha et al., 2000; Varela et al., 2004; Cardinal et al., 2005; De La Rocha, 2006), whereas studies in lacustrine environments are sparse. There are studies linking diatom blooms in lakes with silicon isotope fractionation by seasonal in situ measurements to validate $\delta^{30}Si_{diatom}$ as a bioproductivity proxy (Alleman et al., 2005; Opfergelt et al., 2011; Panizzo et al., 2016). In this context, $\delta^{30}Si_{diatom}$ is used as a paleoenvironmental proxy in a few paleolimnology studies in Asia, for example at Lake El'gygytgyn in North East Siberia (Swann et al., 2010), or in South China (Chen et al., 2012).

Diatoms preferably incorporate light ^{28}Si instead of heavier ^{30}Si (and ^{29}Si) during biomineralization (De La Rocha et al., 1997; Leng et al., 2009). Assuming this fractionation dominates the isotopic signal of the diatoms at Lake Khamra, the decrease of $\delta^{30}Si_{diatom}$ to values of -0.53 ‰ in recent decades contradicts the discussed higher algae productivity in diatom zone 5. Higher bioproductivity increases DSi utilisation and would result in both, an enrichment of the DSi signature of the reservoir (lake water) and of the diatom frustules therein.

https://doi.org/10.5194/egusphere-2024-2470
Preprint. Discussion started: 12 August 2024

In unlimited lake systems, such as Lake Khamra, alteration of DSi sources can influence $\delta^{30}Si_{diatom}$ (Zahajská et al., 2021b), and may overprint the isotopic effect of bioproductivity. We argue that substantial changes in the catchment have led to significant isotopic changes in the reservoir (lake water), which dominate the $\delta^{30}Si_{diatom}$ record at Lake Khamra. Since 1970 CE, both temperature and precipitation increase in the region (Fig. 6), forcing enhanced weathering in the catchment and e.g. leading to a higher nutrient inflow to the lake (Douglas and Smol, 2010), as supported by the increase in OCAR (Fig. 2). In addition, the recent wet and warm period at Lake Khamra follows an earlier dry period around the 1950s with increased wildfire activity in the region (Glückler et al., 2021; Stieg et al., 2024b). Fires in the catchment area have likely altered vegetation and soil conditions, consequently affecting the source of dissolved silica. Soils and terrestrial plants, which tend to have low $\delta^{30}Si_{DSi}$ values (Frings et al., 2016; Sun et al., 2018), may be subject to increased erosion following the (partial) loss of the vegetation cover. Additionally, Lake Khamra lies within a sporadic permafrost zone (Fedorov et al., 2018). Observed warming could increase the depth of the active layer, which as it thaws, would also preferably transport low $\delta^{30}Si_{DSi}$ from litter and soil material into the lake.

Beside the change of catchment supply, an alteration of species composition driven by variations in summer temperatures and the duration of ice–free periods (Zahajská et al., 2021b) could further influence $\delta^{30}Si_{diatom}$. It remains uncertain if a species effect leads to a different silicon isotope fractionation. While Sutton et al. (2013) provided evidence of such effects in marine diatoms, Schmidtbauer et al. (2022) observed varying $\delta^{30}Si_{diatom}$ values in lacustrine samples, which were associated with different preferred habitat regimes. We hypothesise, the $\delta^{30}Si_{diatom}$–decrease at Lake Khamra could hence partially mirror the diatom assemblage change from heavy and compact *Aulacoseira* taxa to less silicified *D. stelligera* and smaller tychoplanktonic and benthic taxa, which have less silicon incorporated.

Overall, interpreting $\delta^{30}Si_{diatom}$ in lacustrine systems is more complex than in marine environments. At Lake Khamra, we consider $\delta^{30}Si_{diatom}$ to be an indicator of weathering rather than of diatom productivity.

4.3.2 Biogeochemical shifts before 1950 CE

Before 1950 CE we observe a prolonged, rather stable period in most biogeochemical proxies (TOC, TN, C/N, OCAR, $\delta^{13}C$, $\delta^{30}Si_{diatom}$; Fig. 2) characterised by a dominance of *Aulacoseira* in diatom zones 2, 3 and 4. The sediment $\delta^{13}C$ values reach up to -30 ‰ and presumably were not substantially influenced by human air pollution prior 1950 CE (Verburg, 2007). The slightly elevated C/N ratio of around 13 indicates a mixed source signal of organic material in combination with the $\delta^{13}C$ values (Fig. A5) as outlined above. However, compared to the period after 1950 CE, there is a tendency towards a more allochthonous origin (Meyers, 2009). On the one hand, there was probably an increased erosional inflow from the catchment due to the higher (winter) precipitation during a rather stable hydroclimatic phase starting in the 1830 CE (Stieg et al., 2024b). On the other hand, only a few species dominated the record at this time (Hill's N2; Fig. 4) and overall low diatom concentrations (DVC) as well as low diatom accumulation rates (DAR; Fig. 4) suggest a reduced lake productivity in comparison with recent decades. Aligned TOC and TN values show their lowest concentration between 1830 and 1950 CE (Fig. 2), indicating reduced bioproductivity (Meyers and Teranes, 2001).

In contrast to low DVC and DAR, observed elevated $\delta^{30}Si_{diatom}$ suggest enhanced bioproductivity based on the classical interpretation of this proxy (De La Rocha et al., 1997). *Aulacoseira* has a high demand of dissolved silica for their heavy and thick frustules, which could have led to a moderate $\delta^{30}Si$ enrichment of the reservoir, but this

https://doi.org/10.5194/egusphere-2024-2470
Preprint. Discussion started: 12 August 2024

is likely a minor effect. We assume that, in contrast to the post–1950s period, the catchment was not yet affected by strong wildfire disturbances, which led to a different source signal pre 1950 CE and hence less weathering and erosional input of soil and plant material with low $\delta^{30}Si_{DSi}$ values is likely. This potentially resulted in a higher $\delta^{30}Si$ level of dissolved silica, which is reflected in the overall elevated $\delta^{30}Si_{diatom}$ and almost constant C/N ratio (Fig. 2). Furthermore, $\delta^{30}Si_{diatom}$ seems rather unaffected by diatom assemblage changes or hydroclimatic variability in the lower part of the core before 1950 CE (as no correlation is observed to any other proxy; Fig. A3), supporting our argumentation whereas we see $\delta^{30}Si_{diatom}$ rather as a weathering proxy at Lake Khamra overprinting the isotopic effect of bioproductivity.

In the early stage of the short core (~ pre 1850 CE) we observe a slight increase of TOC, TN and OCAR (Fig. 2), comparable to recent decades, linked with elevated productivity (Meyers and Teranes, 2001). This overlaps with reconstructed dry and cold conditions (Stieg et al., 2024b), assumed to provide more littoral habitats at a lower lake level (discussed in diatom zone 1), which align with a lower P/B ratio, a reduced abundance of dominant *Aulacoseira* in diatom zone 1 and a simultaneously increased diatom richness (Hill numbers; Fig. 4).

4.4 Ecosystem alterations in Lake Khamra linked to atmospheric pollution

Beside the observed temperature increase due to recent global warming, we observe significant effects of human pollution at Lake Khamra despite its remote location. Mercury concentrations in the lake's sediment increase since the 1950s, with mercury fluxes (HgAR) rapidly rising since the 1990s, which has been primarily linked with human atmospheric pollution (Stieg et al., 2024b). The $\delta^{13}C$ values decline since the 1950s (Fig. 2), partly related to air pollution and the release of light carbon isotopes from burning fossil fuels.

In the same sediment samples, we observe a significant increase in the silicified chrysophyte *Mallomonas* scales (Fig. 4), an indication for lake acidification (Smol et al., 1984) and nutrient load (Munch, 1980). This recent acidification of Lake Khamra is supported by a low pH measurement of 6.07 in the surface water taken in summer 2018 (Stieg et al., 2024b), which is at the minimum range of lakes in the temperate zone with typical taiga vegetation (Pestryakova et al., 2018). Moreover, we observe a strong correlation between HgAR and the *Mallomonas* index after 1950 CE (r 0.92 $p<0.05$; Fig. A4), underlining a trend of long–distance (air)pollution. This acidification tendency is similar to that observed in another pristine lake in south Yakutia (Biskaborn et al., 2021b), where the *Mallomonas* index has also increased in the upper sediment samples.

Lake acidification is a known phenomenon (Farmer, 1990) and is often associated with the formation of S– and N–oxides resulting from the combustion of fossil fuels and thus, from air pollution (Moiseenko and Gashkina, 2011). Atmospheric nutrient enrichment has been reported to increase planktonic pennate diatoms such as *Tabellaria* (Rühland et al., 2015). However, at Lake Khamra we observe a decrease of *T. flocculosa* since 1970 CE, simultaneously with the increase of *D. stelligera* (Fig. 3). The high surface area–to–volume ratio of the cyclotelloid *Discostella* species allows it to sink less rapidly in the photic zone, enhancing light harvesting and nutrient uptake (Smol, 2023). Additionally, this species is known as opportunistic and fast–growing (Rühland et al., 2015; Saros and Anderson, 2015), making it a likely better competitor under changing lake conditions compared to *T. flocculosa*, which thrives in unpolluted lakes (Lange-Bertalot et al., 2017).

Increased abundance of *A. formosa* in oligotrophic alpine lakes in North America is linked to atmospheric N enrichment (Saros et al., 2005; Saros et al., 2010). At Lake Khamra we also observe an increase of planktonic *A. formosa* in the most recent diatom zone 5 (Fig. 3), which could be linked to atmospheric pollution, as the increase

https://doi.org/10.5194/egusphere-2024-2470
Preprint. Discussion started: 12 August 2024

of *Asterionella*, *Fragilaria*, and *Tabellaria* taxa is documented at various locations, not restricted to North America (Rühland et al., 2015). Furthermore, atmospheric pollutants, like reactive N, can accumulate in snow deposits and enter the lake in a pulsed manner through snowmelt (Spaulding et al., 2018). This process affects lakes primarily fed by spring snowmelt (Williams et al., 2009; Spaulding et al., 2018), such as Lake Khamra.

https://doi.org/10.5194/egusphere-2024-2470
Preprint. Discussion started: 12 August 2024

5 Conclusions

Our study of diatom assemblages and biogeochemical proxies from Lake Khamra, eastern Siberia, reveals significant ecosystem changes since circa 1790 CE, likely driven by both hydroclimatic variations and human–induced pollution. Our research addresses a critical gap in lake studies over shorter time periods in Yakutia.

Lake Khamra's diatom assemblage is dominated by a few planktonic diatom species, primarily *Aulacoseira* taxa. At 1970 CE, we observe a drastic shift in the diatom assemblages, characterised mainly by an increase in planktonic *D. stelligera*, while the dominant *Aulacoseira* decrease. We attribute this change to warming, a probable earlier ice–out, and potential summer thermal stratification. These findings are temporally consistent with similar changes observed in temperate lake ecosystems globally.

Carbon and nitrogen records exhibit changes starting in the 1950s, indicating hydroclimatic influence with a delayed shift in the diatom assemblages, which we attribute primarily to rising temperatures and associated effects. At Lake Khamra, $\delta^{30}Si_{diatom}$ appears to reflect weathering rather than diatom productivity. We suggest that wildfire activity in the 1950s, along with increased precipitation and temperatures since 1970 CE, altered silica sources, transporting isotopically light dissolved silica into the lake, which likely led to the observed decrease, overprinting the isotopic effect of bioproductivity.

In addition to elevated mercury levels, determined in a previous study, human impact on the lake ecosystem is evident from fossil fuel–derived $\delta^{13}C$ depletion, pollution–induced changes in diatom species and lake acidification.

These findings underline the dual impact of climate change and anthropogenic pollution on remote lake ecosystems, emphasising the need for comprehensive research to mitigate these effects and protect natural water resources.

https://doi.org/10.5194/egusphere-2024-2470
Preprint. Discussion started: 12 August 2024

Appendix A

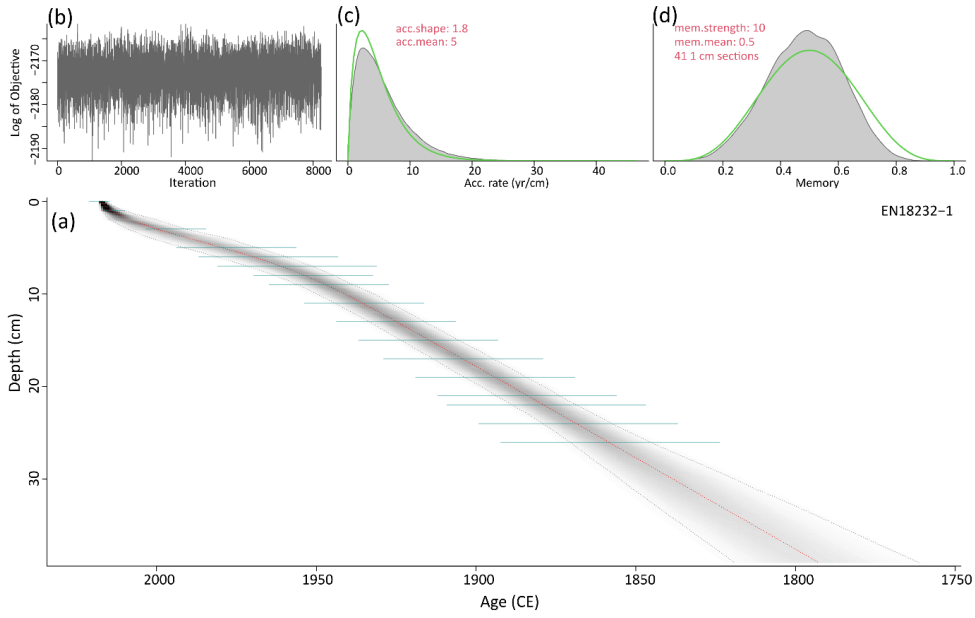

Figure A1. (a) Bayesian accumulation model based on the ^{210}Pb and ^{137}Cs dating (green lines) of the short core EN18232-1 (grey lines indicate the 2σ range; red line indicates the median). (b) Model iteration log. (c, d) Prior (green line) and posterior (grey area) distributions for accumulation rate and memory, respectively. Age–depth model was first published in Stieg et al. (2024b).

https://doi.org/10.5194/egusphere-2024-2470
Preprint. Discussion started: 12 August 2024

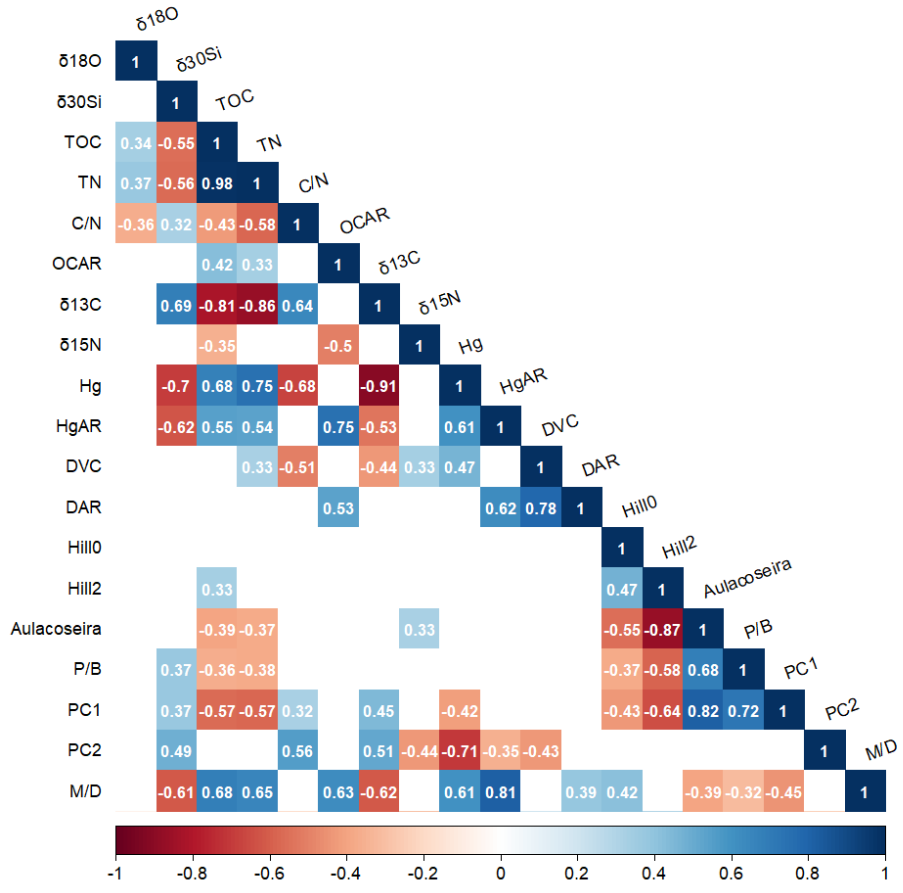

760 **Figure A2. Pearson correlation coefficients of the short core EN18232-1: This matrix displays the Pearson correlation coefficients for selected environmental parameters. The significance threshold for correlation is set at p<0.05, with non–significant correlations being blanked out.**

https://doi.org/10.5194/egusphere-2024-2470
Preprint. Discussion started: 12 August 2024

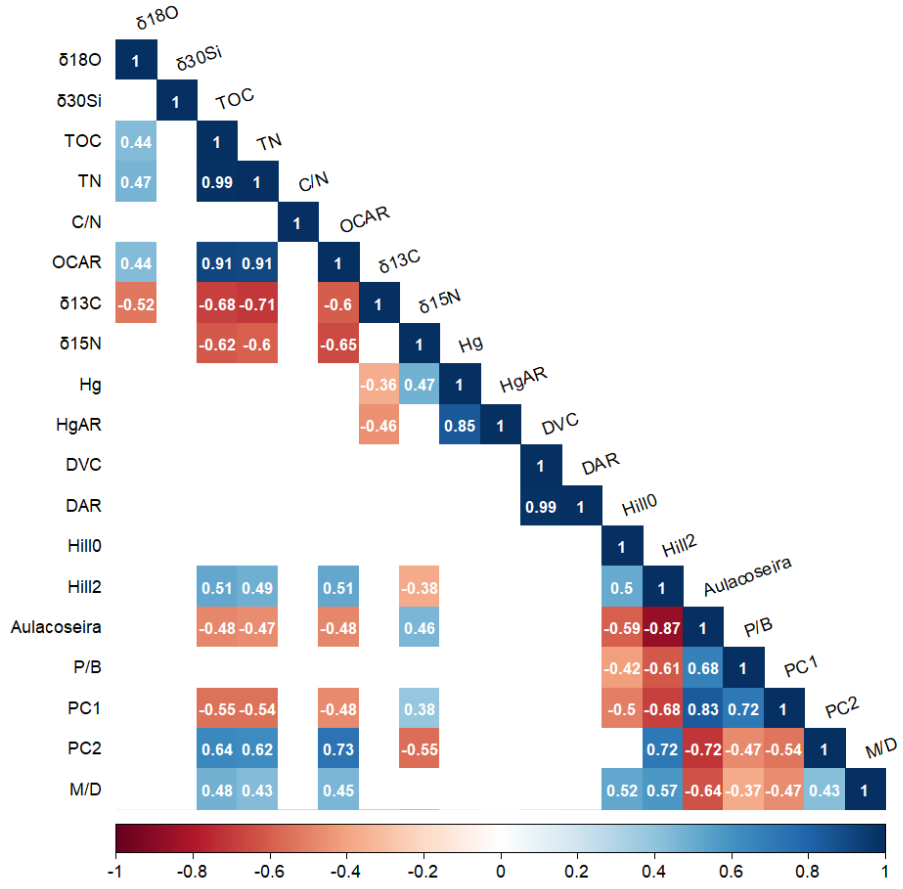

765 **Figure A3. Pearson correlation coefficients pre–1950 CE of the short core EN18232-1: This matrix displays the Pearson correlation coefficients for selected environmental parameters from the period before 1950 CE. The significance threshold for correlation is set at p<0.05, with non–significant correlations being blanked out.**

https://doi.org/10.5194/egusphere-2024-2470
Preprint. Discussion started: 12 August 2024

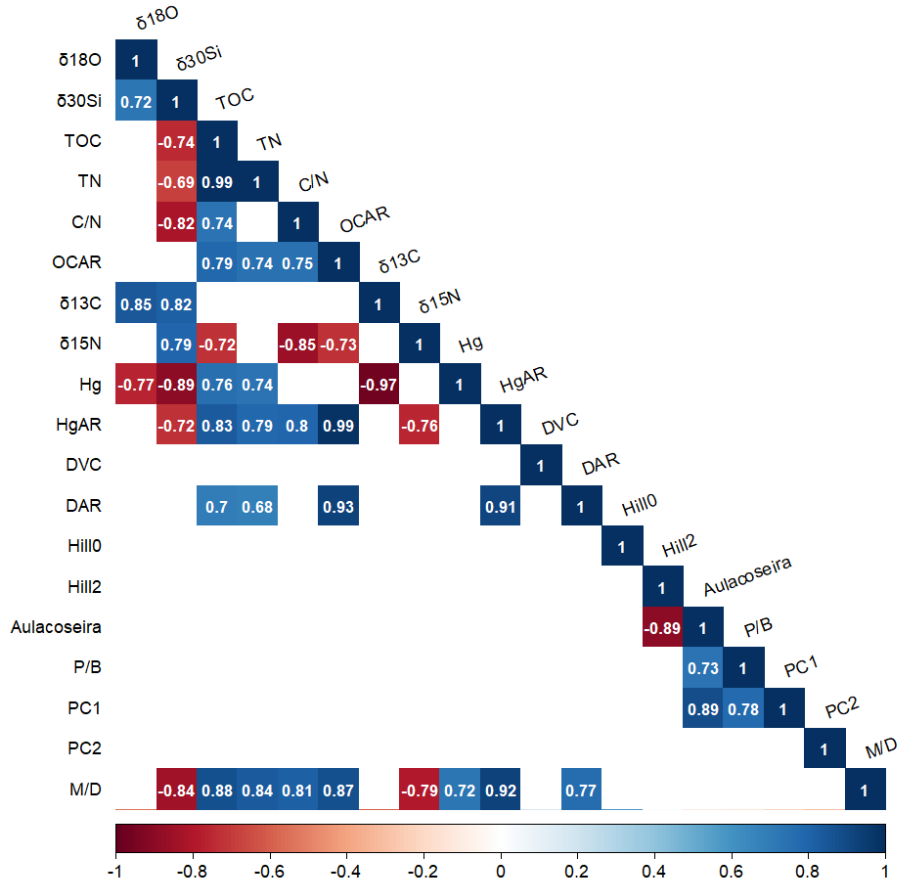

Figure A4. Pearson correlation coefficients past–1950 CE of the short core EN18232-1: This matrix displays the Pearson correlation coefficients for selected environmental parameters from the period after 1950 CE. The significance threshold for correlation is set at p<0.05, with non–significant correlations being blanked out.

https://doi.org/10.5194/egusphere-2024-2470
Preprint. Discussion started: 12 August 2024

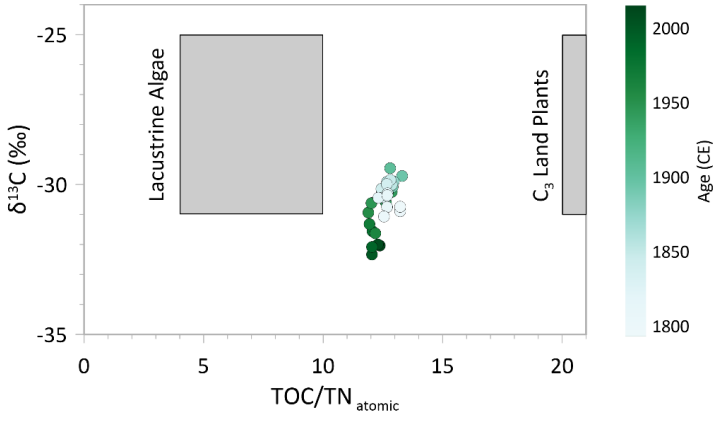

775

Figure A5. C/N–δ^{13}C–plot showing sediment samples of the short core EN18232-1. In general, lacustrine algae have a C/N ratio between 4 to 10, C3 land plants have a ratio > 20 (Meyers and Teranes, 2001). Figure is based on the values given by Meyers and Teranes (2001).

https://doi.org/10.5194/egusphere-2024-2470
Preprint. Discussion started: 12 August 2024

Data availability.

Datasets used in this study are accessible via PANGAEA, including:

1. Diatom assemblage of the sediment short core EN18232-1 and corresponding indices, https://doi.org/10.1594/PANGAEA.971296, Stieg et al. (dataset in review)
2. Diatom silicon isotope record of the sediment short core EN18232-1, https://doi.org/10.1594/PANGAEA.971278, Stieg et al. (dataset in review)
3. Biogeochemical proxies of the sediment short core EN18232-1, https://doi.org/10.1594/PANGAEA.971277, Stieg et al. (dataset in review)

Author contributions.

AS, HM, BKB and UH conceived the study. UH, BKB and LP conducted fieldwork in 2018 and 2020 and received the sediment core. AS processed and analysed the sediment samples in the lab. AS performed diatom analysis and counting, as well as statistical analysis, under the guidance of BKB. AM measured the silicon isotope samples in BHV, with the support of DWD, and helped together with HM to interpret the diatom isotopes. JS supervised the carbon and nitrogen measurements and helped interpret the proxies. AS produced all figures and tables and wrote the manuscript. All authors commented on previous versions of the text and approved the final manuscript.

Competing interests. The authors declare that they have no conflict of interest.

Disclaimer. Colours from the scientific color maps from Crameri et al. (2020) have been used in the figures 3, 4 and 5. Maps throughout this article were created using the Free and Open Source QGIS Geographic Information System. QGIS.org, Version 3.12, 2024.

Acknowledgements. We thank the working groups of the ISOLAB Facility and the CarLa lab of the AWI in Potsdam, as well as the Stable Isotope Facility of the AWI in Bremerhaven. We would further like to thank all participants of the joint German–Russian expedition in Yakutia 2018 and 2020 for their fieldwork.

Financial support. AS is funded by AWI INSPIRES (International Science Program for Integrative Research in Earth Systems).

https://doi.org/10.5194/egusphere-2024-2470
Preprint. Discussion started: 12 August 2024

References

Alleman, L. Y., Cardinal, D., Cocquyt, C., Plisnier, P.-D., Descy, J.-P., Kimirei, I., Sinyinza, D., and André, L.: Silicon Isotopic Fractionation in Lake Tanganyika and Its Main Tributaries, Journal of Great Lakes Research, 31, 509-519, https://doi.org/10.1016/S0380-1330(05)70280-X, 2005.

AMAP: AMAP Arctic Climate Change Update 2021: Key Trends and Impacts. Arctic Monitoring and Assessment Programme (AMAP), Tromsø, Norway, viii+148pp, 978-82-7971-201-5, 2021.

Appleby, P. G., Nolan, P. J., Gifford, D. W., Godfrey, M. J., Oldfield, F., Anderson, N. J., and Battarbee, R. W.: 210Pb dating by low background gamma counting, Hydrobiologia, 143, 21-27, 10.1007/bf00026640, 1986.

Bahls, L. L.: The role of amateurs in modern diatom research, Diatom Research, 30, 209-210, 10.1080/0269249X.2014.988293, 2015.

Barinova, S., Nevo, E., and Bragina, T.: Ecological assessment of wetland ecosystems of northern Kazakhstan on the basis of hydrochemistry and algal biodiversity, Acta Botanica Croatica, 70, 215-244, 10.2478/v10184-010-0020-7, 2011.

Battarbee, R. W. and Kneen, M. J.: The use of electronically counted microspheres in absolute diatom analysis, Limnology and Oceanography, 27, 184-188, 10.4319/lo.1982.27.1.0184, 1982.

Battarbee, R. W., Jones, V. J., Flower, R. J., Cameron, N. G., Bennion, H., Carvalho, L., and Juggins, S.: Diatoms, in: Tracking Environmental Change Using Lake Sediments: Terrestrial, Algal, and Siliceous Indicators, edited by: Smol, J. P., Birks, H. J. B., Last, W. M., Bradley, R. S., and Alverson, K., Springer Netherlands, Dordrecht, 155-202, 10.1007/0-306-47668-1_8, 978-0-306-47668-6, 2001.

Birks, H. J. B.: Numerical methods for the analysis of diatom assemblage data, in: The Diatoms: Applications for the Environmental and Earth Science, edited by: Smol, J. P., and Stoermer, E. F., Cambridge University Press, Cambridge, 23–54, https://doi.org/10.1017/CBO9780511763175, 2010.

Biskaborn, B. K., Herzschuh, U., Bolshiyanov, D., Savelieva, L., and Diekmann, B.: Environmental variability in northeastern Siberia during the last ~ 13,300 yr inferred from lake diatoms and sediment–geochemical parameters, Palaeogeography, Palaeoclimatology, Palaeoecology, 329-330, 22-36, 10.1016/j.palaeo.2012.02.003, 2012.

Biskaborn, B. K., Bolshiyanov, D., Grigoriev, M. N., Morgenstern, A., Pestryakova, L. A., Tsibizov, L., and Dill, A.: Russian-German Cooperation: Expeditions to Siberia in 2020 , Berichte zur Polar- und Meeresforschung = Reports on polar and marine research, Alfred Wegener Institute for Polar and Marine Research, Bremerhaven, 81, 10.48433/BzPM_0756_2021, 2021a.

Biskaborn, B. K., Narancic, B., Stoof-Leichsenring, K. R., Pestryakova, L. A., Appleby, P. G., Piliposian, G. T., and Diekmann, B.: Effects of climate change and industrialization on Lake Bolshoe Toko, eastern Siberia, Journal of Paleolimnology, 65, 335-352, 10.1007/s10933-021-00175-z, 2021b.

Biskaborn, B. K., Forster, A., Pfalz, G., Pestryakova, L. A., Stoof-Leichsenring, K., Strauss, J., Kröger, T., and Herzschuh, U.: Diatom responses and geochemical feedbacks to environmental changes at Lake Rauchuagytgyn (Far East Russian Arctic), Biogeosciences, 20, 1691-1712, 10.5194/bg-20-1691-2023, 2023.

Biskaborn, B. K., Nazarova, L., Kröger, T., Pestryakova, L. A., Syrykh, L., Pfalz, G., Herzschuh, U., and Diekmann, B.: Late Quaternary Climate Reconstruction and Lead-Lag Relationships of Biotic and Sediment-Geochemical Indicators at Lake Bolshoe Toko, Siberia, Frontiers in Earth Science, 9, 737353, 10.3389/feart.2021.737353, 2021c.

Biskaborn, B. K., Subetto, D. A., Savelieva, L. A., Vakhrameeva, P. S., Hansche, A., Herzschuh, U., Klemm, J., Heinecke, L., Pestryakova, L. A., Meyer, H., Kuhn, G., and Diekmann, B.: Late Quaternary vegetation and lake system dynamics in north-eastern Siberia: Implications for seasonal climate variability, Quaternary Science Reviews, 147, 406-421, 10.1016/j.quascirev.2015.08.014, 2016.

Blaauw, M. and Christen, J. A.: Flexible paleoclimate age-depth models using an autoregressive gamma process, Bayesian Analysis, 6, 457-474, 10.1214/11-ba618, 2011.

https://doi.org/10.5194/egusphere-2024-2470
Preprint. Discussion started: 12 August 2024

Cardinal, D., Alleman, L. Y., Dehairs, F., Savoye, N., Trull, T. W., and André, L.: Relevance of silicon isotopes to Si-nutrient utilization and Si-source assessment in Antarctic waters, Global Biogeochemical Cycles, 19, GB2007, 10.1029/2004gb002364, 2005.

Chapligin, B., Meyer, H., Friedrichsen, H., Marent, A., Sohns, E., and Hubberten, H. W.: A high-performance, safer and semi-automated approach for the delta18O analysis of diatom silica and new methods for removing exchangeable oxygen, Rapid Commun Mass Spectrom, 24, 2655-2664, 10.1002/rcm.4689, 2010.

Chelnokova, S. M., Chikina, I. D., and Radchenko, S. A. Geologic map of Yakutia P-48,49, 1 : 1000000, VSEGEI, Leningrad: http://www.geokniga.org/sites/geokniga/, last access: 11. November 2022.

Chen, J., Li, J., Tian, S., Kalugin, I., Darin, A., and Xu, S.: Silicon isotope composition of diatoms as a paleoenvironmental proxy in Lake Huguangyan, South China, Journal of Asian Earth Sciences, 45, 268-274, 10.1016/j.jseaes.2011.11.010, 2012.

Cherapanova, M. V., Snyder, J. A., and Brigham-Grette, J.: Diatom stratigraphy of the last 250 ka at Lake El'gygytgyn, northeast Siberia, Journal of Paleolimnology, 37, 155-162, 10.1007/s10933-006-9019-4, 2006.

Clayton, R. N. and Mayeda, T. K.: The use of bromine pentafluoride in the extraction of oxygen from oxides and silicates for isotopic analysis, Geochim Cosmochim Ac, 27, 43-52, 10.1016/0016-7037(63)90071-1, 1963.

Coddington, O., Lean, J. L., Lindholm, D., Pilewskie, P., Snow, M., and Program, N. C.: NOAA Climate Data Record (CDR) of Total Solar Irradiance (TSI), NRLTSI Version 2 [dataset], 10.7289/V55B00C1 2015.

Crameri, F., Shephard, G. E., and Heron, P. J.: The misuse of colour in science communication, Nat Commun, 11, 5444, 10.1038/s41467-020-19160-7, 2020.

Crutzen, P. J. and Stoermer, E. F.: The "Anthropocene", Global Change Newsletters, 41, 17-18, 0284-5865, 2000.

De La Rocha, C. L.: Opal-based isotopic proxies of paleoenvironmental conditions, Global Biogeochemical Cycles, 20, GB4S09, 10.1029/2005gb002664, 2006.

De La Rocha, C. L., Brzezinski, M. A., and DeNiro, M. J.: Fractionation of silicon isotopes by marine diatoms during biogenic silica formation, Geochim Cosmochim Ac, 61, 5051-5056, Doi 10.1016/S0016-7037(97)00300-1, 1997.

De la Rocha, C. L., Brzezinski, M. A., and DeNiro, M. J.: A first look at the distribution of the stable isotopes of silicon in natural waters, Geochim Cosmochim Ac, 64, 2467-2477, 10.1016/S0016-7037(00)00373-2, 2000.

Dixon, W. J.: Processing Data for Outliers, Biometrics, 9, 74 - 89, 10.2307/3001634, 1953.

Douglas, M. S. V. and Smol, J. P.: Freshwater diatoms as indicators of environmental change in the High Arctic, in: The diatoms: applications for the environmental and earth sciences, edited by: Smol, J. P., and Stoermer, E. F., Cambridge University Press, Cambridge, 249-266, 9780521509961, 2010.

Farmer, A. M.: The effects of lake acidification on aquatic macrophytes--a review, Environ Pollut, 65, 219-240, 10.1016/0269-7491(90)90085-q, 1990.

Fedorov, A., Vasilyev, N., Torgovkin, Y., Shestakova, A., Varlamov, S., Zheleznyak, M., Shepelev, V., Konstantinov, P., Kalinicheva, S., Basharin, N., Makarov, V., Ugarov, I., Efremov, P., Argunov, R., Egorova, L., Samsonova, V., Shepelev, A., Vasiliev, A., Ivanova, R., Galanin, A., Lytkin, V., Kuzmin, G., and Kunitsky, V.: Permafrost-Landscape Map of the Republic of Sakha (Yakutia) on a Scale 1:1,500,000, Geosciences, 8, 465 - 481, 10.3390/geosciences8120465, 2018.

Firsova, A. D., Chebykin, E. P., Kopyrina, L. I., Rodionova, E. V., Chensky, D. A., Gubin, N. A., Panov, V. S., Pogodaeva, T. V., Bukin, Y. S., Suturin, A. N., and Likhoshway, Y. V.: Post-glacial diatom and geochemical records of ecological status and water level changes of Lake Vorota, Western Beringia, Journal of Paleolimnology, 66, 407-437, 10.1007/s10933-021-00214-9, 2021.

https://doi.org/10.5194/egusphere-2024-2470
Preprint. Discussion started: 12 August 2024

Frings, P. J., Clymans, W., Fontorbe, G., De La Rocha, C. L., and Conley, D. J.: The continental Si cycle and its impact on the ocean Si isotope budget, Chemical Geology, 425, 12-36, 10.1016/j.chemgeo.2016.01.020, 2016.

Geng, R., Andreev, A., Kruse, S., Heim, B., van Geffen, F., Pestryakova, L., Zakharov, E., Troeva, E., Shevtsova, I., Li, F., Zhao, Y., and Herzschuh, U.: Modern Pollen Assemblages From Lake Sediments and Soil in East Siberia and Relative Pollen Productivity Estimates for Major Taxa, Frontiers in Ecology and Evolution, 10, 837857, 10.3389/fevo.2022.837857, 2022.

Gibson, C. E., Anderson, N. J., and Haworth, E. Y.: Aulacoseira subarctica: taxonomy, physiology, ecology and palaeoecology, European Journal of Phycology, 38, 83-101, 10.1080/0967026031000094102, 2003.

Glückler, R., Herzschuh, U., Kruse, S., Andreev, A., Vyse, S. A., Winkler, B., Biskaborn, B. K., Pestryakova, L., and Dietze, E.: Wildfire history of the boreal forest of south-western Yakutia (Siberia) over the last two millennia documented by a lake-sediment charcoal record, Biogeosciences, 18, 4185-4209, 10.5194/bg-18-4185-2021, 2021.

Gorokhov, A. N. and Fedorov, A. N.: Current Trends in Climate Change in Yakutia, Geography and Natural Resources, 39, 153-161, 10.1134/s1875372818020087, 2018.

Grimm, E. C.: Coniss - a Fortran-77 Program for Stratigraphically Constrained Cluster-Analysis by the Method of Incremental Sum of Squares, Comput Geosci, 13, 13-35, 10.1016/0098-3004(87)90022-7, 1987.

Guiry, M. D. and Guiry, G. M. AlgaeBase. World-wide electronic publication, National University of Ireland, Galway.: https://www.algaebase.org, last access: 1. August 2024.

Häkansson, H. and Kling, H.: A light and electron microscope study of previously described and new Stephanodiscus species (bacillariophyceae) from central and northern Canadian lakes, with ecological notes on the species, Diatom Research, 4, 269-288, 10.1080/0269249X.1989.9705076, 1989.

Heudre, D., Wetzel, C. E., Lange-Bertalot, H., Van de Vijver, B., Moreau, L., and Ector, L.: A review of Tabellaria species from freshwater environments in Europe, Fottea, 21, 180-205, 10.5507/fot.2021.005, 2021.

Hofmann, G., Lange-Bertalot, H., and Werum, M.: Diatomeen im Süßwasser-Benthos von Mitteleuropa: Bestimmungsflora Kieselalgen für die ökologische Praxis; über 700 der häufigsten Arten und ihre Ökologie, A.R.G. Gantner Verlag K.G., 908 pp., 9783906166926, 2011.

Horn, H., Paul, L., Horn, W., and Petzoldt, T.: Long-term trends in the diatom composition of the spring bloom of a German reservoir: is Aulacoseira subarctica favoured by warm winters?, Freshwater Biology, 56, 2483-2499, 10.1111/j.1365-2427.2011.02674.x, 2011.

Huang, S., Zhang, K., Lin, Q., Liu, J., and Shen, J.: Abrupt ecological shifts of lakes during the Anthropocene, Earth-Science Reviews, 227, 103981, 10.1016/j.earscirev.2022.103981, 2022.

Jasinski, J. P. P., Warner, B. G., Andreev, A. A., Aravena, R., Gilbert, S. E., Zeeb, B. A., Smol, J. P., and Velichko, A. A.: Holocene environmental history of a peatland in the Lena River valley, Siberia, Canadian Journal of Earth Sciences, 35, 637-648, 10.1139/e98-015, 1998.

Jiang, S., Liu, X., Sun, J., Yuan, L., Sun, L., and Wang, Y.: A multi-proxy sediment record of late Holocene and recent climate change from a lake near Ny-Ålesund, Svalbard, Boreas, 40, 468-480, 10.1111/j.1502-3885.2010.00198.x, 2011.

Jones, V. J., Rose, N. L., Self, A. E., Solovieva, N., and Yang, H.: Evidence of global pollution and recent environmental change in Kamchatka, Russia, Global and Planetary Change, 134, 82-90, 10.1016/j.gloplacha.2015.02.005, 2015.

Juggins, S. Rioja: Analysis of Quaternary Science Data, R package: https://cran.r-project.org/package=rioja, last access: 25. February 2024.

Kahlert, M., Rühland, K. M., Lavoie, I., Keck, F., Saulnier-Talbot, E., Bogan, D., Brua, R. B., Campeau, S., Christoffersen, K. S., Culp, J. M., Karjalainen, S. M., Lento, J., Schneider, S. C., Shaftel, R., and

https://doi.org/10.5194/egusphere-2024-2470
Preprint. Discussion started: 12 August 2024

Smol, J. P.: Biodiversity patterns of Arctic diatom assemblages in lakes and streams: Current reference conditions and historical context for biomonitoring, Freshwater Biology, 67, 116-140, 10.1111/fwb.13490, 2020.

Keeling, C. D.: The Suess effect: 13Carbon-14Carbon interrelations, Environment International, 2, 229-300, 10.1016/0160-4120(79)90005-9, 1979.

Kirillina, K., Shvetsov, E. G., Protopopova, V. V., Thiesmeyer, L., and Yan, W.: Consideration of anthropogenic factors in boreal forest fire regime changes during rapid socio-economic development: case study of forestry districts with increasing burnt area in the Sakha Republic, Russia, Environmental Research Letters, 15, 035009, 10.1088/1748-9326/ab6c6e, 2020.

Klein Tank, A. M. G., Wijngaard, J. B., Können, G. P., Böhm, R., Demarée, G., Gocheva, A., Mileta, M., Pashiardis, S., Hejkrlik, L., Kern-Hansen, C., Heino, R., Bessemoulin, P., Müller-Westermeier, G., Tzanakou, M., Szalai, S., Pálsdóttir, T., Fitzgerald, D., Rubin, S., Capaldo, M., Maugeri, M., Leitass, A., Bukantis, A., Aberfeld, R., van Engelen, A. F. V., Forland, E., Mietus, M., Coelho, F., Mares, C., Razuvaev, V., Nieplova, E., Cegnar, T., Antonio López, J., Dahlström, B., Moberg, A., Kirchhofer, W., Ceylan, A., Pachaliuk, O., Alexander, L. V., and Petrovic, P.: Daily dataset of 20th-century surface air temperature and precipitation series for the European Climate Assessment, International Journal of Climatology, 22, 1441-1453, 10.1002/joc.773, 2002.

Kostrova, S. S., Biskaborn, B. K., Pestryakova, L. A., Fernandoy, F., Lenz, M. M., and Meyer, H.: Climate and environmental changes of the Lateglacial transition and Holocene in northeastern Siberia: Evidence from diatom oxygen isotopes and assemblage composition at Lake Emanda, Quaternary Science Reviews, 259, 106905, 10.1016/j.quascirev.2021.106905, 2021.

Krammer, K. and Lange-Bertalot, H.: Bacillariophyceae, 4. Teil: Achnanthaceae, Kritische Ergänzungen zu Navicula (Lineolatae) und Gomphonema, Gesamtliteraturverzeichnis Teil 1 - 4, Süßwasserflora von Mitteleuropa, Band 2/4, Gustav Fischer Verlag, Stuttgart, Jena, 3437306642, 1991.

Krammer, K. and Lange-Bertalot, H.: Bacillariophyceae, 2. Teil: Bacillariaceae, Epithemiaceae, Surirellaceae, Süßwasserflora von Mitteleuropa, Band 2/2, Gustav Fischer Verlag, Jena, 3437353888, 1997a.

Krammer, K. and Lange-Bertalot, H.: Bacillariophyceae, 1. Teil: Naviculaceae, Süßwasserflora von Mitteleuropa, Band 2/1, Gustav Fischer Verlag, Jena, 3437353969, 1997b.

Krammer, K., Lange-Bertalot, H., Håkansson, H., and Nörpel, M.: Bacillariophyceae, 3. Teil: Centrales, Fragilariaceae, Eunotiaceae, Süßwasserflora von Mitteleuropa, Band 2/3, Gustav Fischer Verlag, Stuttgart, Jena, 3437305417, 1991.

Kruse, S., Bolshiyanov, D., Grigoriev, M. N., Morgenstern, A., Pestryakova, L., Tsibizov, L., and Udke, A.: Russian-German Cooperation: Expeditions to Siberia in 2018, Alfred Wegener Institute for Polar and Marine Research, Bremerhaven, 263, https://doi.org/10.2312/BzPM_0734_2019, 2019.

Laing, T. E. and Smol, J. P.: Late Holocene environmental changes inferred from diatoms in a lake on the western Taimyr Peninsula, northern Russia, Journal of Paleolimnology, 30, 231-247, 0.1023/A:1025561905506, 2003.

Lange-Bertalot, H., Hofmann, G., Werum, M., and Cantonati, M., Cantonati, M., Kelly, M. G., and Lange-Bertalot, H. (Eds.): Freshwater benthic diatoms of Central Europe : over 800 common species used in ecological assessment, Koeltz Botanical Books, Schmitten-Oberreifenberg/Germany, 942 pp., 978-3-946583-06-6, 2017.

Leng, M. J. and Barker, P. A.: A review of the oxygen isotope composition of lacustrine diatom silica for palaeoclimate reconstruction, Earth-Science Reviews, 75, 5-27, 10.1016/j.earscirev.2005.10.001, 2006.

Leng, M. J. and Sloane, H. J.: Combined oxygen and silicon isotope analysis of biogenic silica, Journal of Quaternary Science, 23, 313-319, 10.1002/jqs.1177, 2008.

https://doi.org/10.5194/egusphere-2024-2470
Preprint. Discussion started: 12 August 2024

Leng, M. J., Swann, G. E. A., Hodson, M. J., Tyler, J. J., Patwardhan, S. V., and Sloane, H. J.: The Potential use of Silicon Isotope Composition of Biogenic Silica as a Proxy for Environmental Change, Silicon, 1, 65-77, 10.1007/s12633-009-9014-2, 2009.

Mackay, A. W., Felde, V. A., Morley, D. W., Piotrowska, N., Rioual, P., Seddon, A. W. R., and Swann, G. E. A.: Long-term trends in diatom diversity and palaeoproductivity: a 16 000-year multidecadal record from Lake Baikal, southern Siberia, Clim Past, 18, 363-380, 10.5194/cp-18-363-2022, 2022.

Maier, E., Chapligin, B., Abelmann, A., Gersonde, R., Esper, O., Ren, J., Friedrichsen, H., Meyer, H., and Tiedemann, R.: Combined oxygen and silicon isotope analysis of diatom silica from a deglacial subarctic Pacific record, Journal of Quaternary Science, 28, 571-581, 10.1002/jqs.2649, 2013.

Messager, M. L., Lehner, B., Grill, G., Nedeva, I., and Schmitt, O.: Estimating the volume and age of water stored in global lakes using a geo-statistical approach, Nat Commun, 7, 13603, 10.1038/ncomms13603, 2016.

Meyers, P. A.: Organic Geochemical Proxies, in: Encyclopedia of Paleoclimatology and Ancient Environments. Encyclopedia of Earth Sciences Series., edited by: Gornitz, V., Springer, Dordrecht, 659–663, https://doi.org/10.1007/978-1-4020-4411-3_160, 978-1-4020-4551-6, 2009.

Meyers, P. A. and Teranes, J. L.: Sediment Organic Matter, in: Tracking environmental change using lake sediments. Volume 2: Physical and Geochemical Methods., edited by: Last, W. M., and Smol, J. P., Kluwer Academic Publishers, The Netherlands, 239-269, 1402006284, 2001.

Michelutti, N., Cooke, C. A., Hobbs, W. O., and Smol, J. P.: Climate-driven changes in lakes from the Peruvian Andes, Journal of Paleolimnology, 54, 153-160, 10.1007/s10933-015-9843-5, 2015.

Miesner, T., Herzschuh, U., Pestryakova, L. A., Wieczorek, M., Zakharov, E. S., Kolmogorov, A. I., Davydova, P. V., and Kruse, S.: Forest structure and individual tree inventories of northeastern Siberia along climatic gradients, Earth Syst. Sci. Data, 14, 5695-5716, 10.5194/essd-14-5695-2022, 2022.

Moiseenko, T. I. and Gashkina, N. A.: Zonal features of lake acidification, Water Resources, 38, 47-62, 10.1134/s0097807811010076, 2011.

Moos, M. T., Laird, K. R., and Cumming, B. F.: Climate-related eutrophication of a small boreal lake in northwestern Ontario: a palaeolimnological perspective, Holocene, 19, 359-367, 10.1177/0959683608101387, 2009.

Morley, D. W., Leng, M. J., Mackay, A. W., Sloane, H. J., Rioual, P., and Battarbee, R. W.: Cleaning of lake sediment samples for diatom oxygen isotope analysis, Journal of Paleolimnology, 31, 391-401, 10.1023/B:JOPL.0000021854.70714.6b, 2004.

Munch, C. S.: Fossil diatoms and scales of Chrysophyceae in the recent history of Hall Lake, Washington, Freshwater Biology, 10, 61-66, 10.1111/j.1365-2427.1980.tb01180.x, 1980.

Narancic, B., Pienitz, R., Chapligin, B., Meyer, H., Francus, P., and Guilbault, J.-P.: Postglacial environmental succession of Nettilling Lake (Baffin Island, Canadian Arctic) inferred from biogeochemical and microfossil proxies, Quaternary Science Reviews, 147, 391-405, 10.1016/j.quascirev.2015.12.022, 2016.

Obu, J., Westermann, S., Bartsch, A., Berdnikov, N., Christiansen, H. H., Dashtseren, A., Delaloye, R., Elberling, B., Etzelmüller, B., Kholodov, A., Khomutov, A., Kääb, A., Leibman, M. O., Lewkowicz, A. G., Panda, S. K., Romanovsky, V., Way, R. G., Westergaard-Nielsen, A., Wu, T., Yamkhin, J., and Zou, D.: Northern Hemisphere permafrost map based on TTOP modelling for 2000–2016 at 1 km2 scale, Earth-Science Reviews, 193, 299-316, 10.1016/j.earscirev.2019.04.023, 2019.

Oksanen, J., Simpson, G., Blanchet, F., Kindt, R., Legendre, P., Minchin, P., O'Hara, R., Solymos, P., Stevens, M., Szoecs, E., Wagner, H., Barbour, M., Bedward, M., Bolker, B., Borcard, D., Carvalho, G., Chirico, M., De Caceres, M., Durand, S., Evangelista, H., FitzJohn, R., Friendly, M., Furneaux, B., Hannigan, G., Hill, M., Lahti, L., McGlinn, D., Ouellette, M., Ribeiro Cunha, E., Smith, T., Stier, A., Ter Braak, C., and Weedon, J. Vegan: Community Ecology Package. R package version 2.6-4: https://CRAN.R-project.org/package=vegan, last access: 14. March 2024.

https://doi.org/10.5194/egusphere-2024-2470
Preprint. Discussion started: 12 August 2024

Opfergelt, S., Eiriksdottir, E. S., Burton, K. W., Einarsson, A., Siebert, C., Gislason, S. R., and Halliday, A. N.: Quantifying the impact of freshwater diatom productivity on silicon isotopes and silicon fluxes: Lake Myvatn, Iceland, Earth and Planetary Science Letters, 305, 73-82, 10.1016/j.epsl.2011.02.043, 2011.

Palagushkina, O., Nazarova, L., and Frolova, L.: Trends in development of diatom flora from sub-recent lake sediments of the Lake Bolshoy Kharbey (Bolshezemelskaya tundra, Russia), Biological Communications, 64, 244–251, 10.21638/spbu03.2019.403, 2020.

Palagushkina, O. V., Nazarova, L. B., Wetterich, S., and Schirrmeister, L.: Diatoms of modern bottom sediments in Siberian arctic, Contemporary Problems of Ecology, 5, 413-422, 10.1134/s1995425512040105, 2012.

Panizzo, V. N., Swann, G. E. A., Mackay, A. W., Vologina, E., Sturm, M., Pashley, V., and Horstwood, M. S. A.: Insights into the transfer of silicon isotopes into the sediment record, Biogeosciences, 13, 147-157, 10.5194/bg-13-147-2016, 2016.

Pestryakova, L. A., Herzschuh, U., Gorodnichev, R., and Wetterich, S.: The sensitivity of diatom taxa from Yakutian lakes (north-eastern Siberia) to electrical conductivity and other environmental variables, Polar Research, 37, 1485625, 10.1080/17518369.2018.1485625, 2018.

Pestryakova, L. A., Herzschuh, U., Wetterich, S., and Ulrich, M.: Present-day variability and Holocene dynamics of permafrost-affected lakes in central Yakutia (Eastern Siberia) inferred from diatom records, Quaternary Science Reviews, 51, 56-70, 10.1016/j.quascirev.2012.06.020, 2012.

Philibert, A., Prairie, Y. T., Campbell, I., and Laird, L.: Effects of late Holocene wildfires on diatom assemblages in Christina Lake, Alberta, Canada, Canadian Journal of Forest Research, 33, 2405-2415, 10.1139/x03-165, 2003.

R Core Team. R: A Language and Environment for Statistical Computing, R version 4.4.1: https://www.R-project.org/, last access: 2024.

Reynolds, C. S., Huszar, V., Kruk, C., Naselli-Flores, L., and Melo, S.: Towards a functional classification of the freshwater phytoplankton, J Plankton Res, 24, 417-428, 10.1093/plankt/24.5.417, 2002.

Rimet, F., Druart, J.-C., and Anneville, O.: Exploring the dynamics of plankton diatom communities in Lake Geneva using emergent self-organizing maps (1974–2007), Ecological Informatics, 4, 99-110, 10.1016/j.ecoinf.2009.01.006, 2009.

Roberts, S. L., Swann, G. E. A., McGowan, S., Panizzo, V. N., Vologina, E. G., Sturm, M., and Mackay, A. W.: Diatom evidence of 20th century ecosystem change in Lake Baikal, Siberia, PLoS One, 13, e0208765, 10.1371/journal.pone.0208765, 2018.

Rühland, K. and Smol, J. P.: Diatom shifts as evidence for recent Subarctic warming in a remote tundra lake, NWT, Canada, Palaeogeography, Palaeoclimatology, Palaeoecology, 226, 1-16, 10.1016/j.palaeo.2005.05.001, 2005.

Rühland, K., Paterson, A. M., and Smol, J. P.: Hemispheric-scale patterns of climate-related shifts in planktonic diatoms from North American and European lakes, Global Change Biology, 14, 2740-2754, 10.1111/j.1365-2486.2008.01670.x, 2008.

Rühland, K., Priesnitz, A., and Smol, J. P.: Paleolimnological Evidence from Diatoms for Recent Environmental Changes in 50 Lakes across Canadian Arctic Treeline, Arctic, Antarctic, and Alpine Research, 35, 110-123, 10.1657/1523-0430(2003)035[0110:Pefdfr]2.0.Co;2, 2003.

Rühland, K., Smol, J. P., Jasinski, J. P. P., and Warner, B. G.: Response of Diatoms and Other Siliceous Indicators to the Developmental History of a Peatland in the Tiksi Forest, Siberia, Russia, Arctic, Antarctic, and Alpine Research, 32, 167-178, 10.1080/15230430.2000.12003352, 2000.

Rühland, K. M., Paterson, A. M., and Smol, J. P.: Lake diatom responses to warming: reviewing the evidence, Journal of Paleolimnology, 54, 1-35, 10.1007/s10933-015-9837-3, 2015.

https://doi.org/10.5194/egusphere-2024-2470
Preprint. Discussion started: 12 August 2024

Rühland, K. M., Paterson, A. M., Keller, W., Michelutti, N., and Smol, J. P.: Global warming triggers the loss of a key Arctic refugium, Proc Biol Sci, 280, 20131887, 10.1098/rspb.2013.1887, 2013.

Ryves, D. B., Juggins, S., Fritz, S. C., and Battarbee, R. W.: Experimental diatom dissolution and the quantification of microfossil preservation in sediments, Palaeogeogr Palaeocl, 172, 99-113, 10.1016/S0031-0182(01)00273-5, 2001.

Saros, J. E. and Anderson, N. J.: The ecology of the planktonic diatom Cyclotella and its implications for global environmental change studies, Biol Rev Camb Philos Soc, 90, 522-541, 10.1111/brv.12120, 2015.

Saros, J. E., Michel, T. J., Interlandi, S. J., and Wolfe, A. P.: Resource requirements of Asterionella formosa and Fragilaria crotonensis in oligotrophic alpine lakes: implications for recent phytoplankton community reorganizations, Canadian Journal of Fisheries and Aquatic Sciences, 62, 1681-1689, 10.1139/f05-077, 2005.

Saros, J. E., Rose, K. C., Clow, D. W., Stephens, V. C., Nurse, A. B., Arnett, H. A., Stone, J. R., Williamson, C. E., and Wolfe, A. P.: Melting Alpine Glaciers Enrich High-Elevation Lakes with Reactive Nitrogen, Environmental Science & Technology, 44, 4891-4896, 10.1021/es100147j, 2010.

Schmidtbauer, K., Noble, P., Rosen, M., Conley, D. J., and Frings, P. J.: Linking silicon isotopic signatures with diatom communities, Geochim Cosmochim Ac, 323, 102-122, 10.1016/j.gca.2022.02.015, 2022.

Shestakova, A. A., Fedorov, A. N., Torgovkin, Y. I., Konstantinov, P. Y., Vasyliev, N. F., Kalinicheva, S. V., Samsonova, V. V., Hiyama, T., Iijima, Y., Park, H., Iwahana, G., and Gorokhov, A. N.: Mapping the Main Characteristics of Permafrost on the Basis of a Permafrost-Landscape Map of Yakutia Using GIS, Land, 10, 10.3390/land10050462, 2021.

Smol, J. P.: Lakes in the Anthropocene: Reflections on tracking ecosystem change in the Arctic., International Ecology Institute, Oldendorf/Luhe, Germany, 438 pp., https://doi.org/10.1002/lob.10634, 978-3-946729-30-3, 2023.

Smol, J. P. and Douglas, M. S. V.: From controversy to consensus: making the case for recent climate change in the Arctic using lake sediments, Frontiers in Ecology and the Environment, 5, 466-474, 10.1890/060162, 2007.

Smol, J. P. and Stoermer, E. F.: The diatoms: applications for the environmental and earth sciences, Cambridge University Press, Cambridge, New York, Melbourne, Madrid, Cape Town, Singepore, São Paulo, Dehli, Dubai, Tokyo, Mexico City, 687 pp., 9780521509961, 2010.

Smol, J. P., Charles, D., and DR, W.: Mallomonadacean microfossil provide evidence of recent lake acidification, Nature, 307, 628-630, 1984.

Smol, J. P., Wolfe, A. P., Birks, H. J., Douglas, M. S., Jones, V. J., Korhola, A., Pienitz, R., Ruhland, K., Sorvari, S., Antoniades, D., Brooks, S. J., Fallu, M. A., Hughes, M., Keatley, B. E., Laing, T. E., Michelutti, N., Nazarova, L., Nyman, M., Paterson, A. M., Perren, B., Quinlan, R., Rautio, M., Saulnier-Talbot, E., Siitonen, S., Solovieva, N., and Weckstrom, J.: Climate-driven regime shifts in the biological communities of arctic lakes, Proc Natl Acad Sci U S A, 102, 4397-4402, 10.1073/pnas.0500245102, 2005.

Sochuliakova, L., Sienkiewicz, E., Hamerlik, L., Svitok, M., Fidlerova, D., and Bitusik, P.: Reconstructing the Trophic History of an Alpine Lake (High Tatra Mts.) Using Subfossil Diatoms: Disentangling the Effects of Climate and Human Influence, Water Air Soil Pollut, 229, 289, 10.1007/s11270-018-3940-9, 2018.

Solovieva, N., Jones, V., Birks, J. H. B., Appleby, P., and Nazarova, L.: Diatom responses to 20th century climate warming in lakes from the northern Urals, Russia, Palaeogeography, Palaeoclimatology, Palaeoecology, 259, 96-106, 10.1016/j.palaeo.2007.10.001, 2008.

Sorvari, S., Korhola, A., and Thompson, R.: Lake diatom response to recent Arctic warming in Finnish Lapland, Global Change Biology, 8, 171-181, 10.1046/j.1365-2486.2002.00463.x, 2002.

https://doi.org/10.5194/egusphere-2024-2470
Preprint. Discussion started: 12 August 2024

Spaulding, S. A., Otu, M. K., Wolfe, A. P., and Baron, J. S.: Paleolimnological Records of Nitrogen Deposition in Shallow, High-Elevation Lakes of Grand Teton National Park, Wyoming, U.S.A, Arctic, Antarctic, and Alpine Research, 47, 703-717, 10.1657/aaar0015-008, 2018.

Spaulding, S. A., Potapova, M. G., Bishop, I. W., Lee, S. S., Gasperak, T. S., Jovanoska, E., Furey, P. C., and Edlund, M. B.: Diatoms.org: supporting taxonomists, connecting communities, Diatom Research, 36, 291-304, 10.1080/0269249X.2021.2006790, 2021.

Steffen, W., Broadgate, W., Deutsch, L., Gaffney, O., and Ludwig, C.: The trajectory of the Anthropocene: The Great Acceleration, The Anthropocene Review, 2, 81-98, 10.1177/2053019614564785, 2015.

Stevenson, M. A., McGowan, S., Pearson, E. J., Swann, G. E. A., Leng, M. J., Jones, V. J., Bailey, J. J., Huang, X., and Whiteford, E.: Anthropocene climate warming enhances autochthonous carbon cycling in an upland Arctic lake, Disko Island, West Greenland, Biogeosciences, 18, 2465-2485, 10.5194/bg-18-2465-2021, 2021.

Stieg, A., Biskaborn, B. K., Herzschuh, U., Strauss, J., Lindemann, J., and Meyer, H.: Mercury from sediment short core EN18232-1 of Lake Khamra, SW Yakutia, Siberia, Russia. [dataset], https://doi.org/10.1594/PANGAEA.962973, 2024a.

Stieg, A., Biskaborn, B. K., Herzschuh, U., Strauss, J., Pestryakova, L., and Meyer, H.: Hydroclimatic anomalies detected by a sub-decadal diatom oxygen isotope record of the last 220 years from Lake Khamra, Siberia, Clim. Past, 20, 909-933, 10.5194/cp-20-909-2024, 2024b.

Sun, X., Mörth, C.-M., Porcelli, D., Kutscher, L., Hirst, C., Murphy, M. J., Maximov, T., Petrov, R. E., Humborg, C., Schmitt, M., and Andersson, P. S.: Stable silicon isotopic compositions of the Lena River and its tributaries: Implications for silicon delivery to the Arctic Ocean, Geochim Cosmochim Ac, 241, 120-133, 10.1016/j.gca.2018.08.044, 2018.

Sutton, J. N., Varela, D. E., Brzezinski, M. A., and Beucher, C. P.: Species-dependent silicon isotope fractionation by marine diatoms, Geochim Cosmochim Ac, 104, 300-309, 10.1016/j.gca.2012.10.057, 2013.

Sutton, J. N., André, L., Cardinal, D., Conley, D. J., de Souza, G. F., Dean, J., Dodd, J., Ehlert, C., Ellwood, M. J., Frings, P. J., Grasse, P., Hendry, K., Leng, M. J., Michalopoulos, P., Panizzo, V. N., and Swann, G. E. A.: A Review of the Stable Isotope Bio-geochemistry of the Global Silicon Cycle and Its Associated Trace Elements, Frontiers in Earth Science, 5:112, 10.3389/feart.2017.00112, 2018.

Swann, G. E. A., Leng, M. J., Juschus, O., Melles, M., Brigham-Grette, J., and Sloane, H. J.: A combined oxygen and silicon diatom isotope record of Late Quaternary change in Lake El'gygytgyn, North East Siberia, Quaternary Science Reviews, 29, 774-786, 10.1016/j.quascirev.2009.11.024, 2010.

Varela, D. E., Pride, C. J., and Brzezinski, M. A.: Biological fractionation of silicon isotopes in Southern Ocean surface waters, Global Biogeochemical Cycles, 18, GB1047, 10.1029/2003gb002140, 2004.

Verburg, P.: The need to correct for the Suess effect in the application of δ13C in sediment of autotrophic Lake Tanganyika, as a productivity proxy in the Anthropocene, Journal of Paleolimnology, 37, 591-602, 10.1007/s10933-006-9056-z, 2007.

Wang, L., Rioual, P., Panizzo, V. N., Lu, H., Gu, Z., Chu, G., Yang, D., Han, J., Liu, J., and Mackay, A. W.: A 1000-yr record of environmental change in NE China indicated by diatom assemblages from maar lake Erlongwan, Quaternary Research, 78, 24-34, 10.1016/j.yqres.2012.03.006, 2012.

Wei, T. and Simko, V. R package 'corrplot': Visualization of a Correlation Matrix. (Version 0.92): https://github.com/taiyun/corrplot, last access: 25. February 2024.

Williams, M. W., Seibold, C., and Chowanski, K.: Storage and release of solutes from a subalpine seasonal snowpack: soil and stream water response, Niwot Ridge, Colorado, Biogeochemistry, 95, 77-94, 10.1007/s10533-009-9288-x, 2009.

Wolin, J. A. and Stone, J. R.: Diatoms as Indicators of Water-level Change in Freshwater Lakes, in: The Diatoms Applications to the Environmental and Earth Sciences, edited by: Stoermer, E. F., and Smol, J. P., Cambridge University Press., 174-185, 2010.

https://doi.org/10.5194/egusphere-2024-2470
Preprint. Discussion started: 12 August 2024

Yan, Y., Wang, L., Li, J., Li, J., Zou, Y., Zhang, J., Li, P., Liu, Y., Xu, B., Gu, Z., and Wan, X.: Diatom response to climatic warming over the last 200 years: A record from Gonghai Lake, North China, Palaeogeography, Palaeoclimatology, Palaeoecology, 495, 48-59, 10.1016/j.palaeo.2017.12.023, 2018.

Zahajská, P., Olid, C., Stadmark, J., Fritz, S. C., Opfergelt, S., and Conley, D. J.: Modern silicon dynamics of a small high-latitude subarctic lake, Biogeosciences, 18, 2325-2345, 10.5194/bg-18-2325-2021, 2021a.

Zahajská, P., Cartier, R., Fritz, S. C., Stadmark, J., Opfergelt, S., Yam, R., Shemesh, A., and Conley, D. J.: Impact of Holocene climate change on silicon cycling in Lake 850, Northern Sweden, The Holocene, 31, 1582-1592, 10.1177/09596836211025973, 2021b.

Zalasiewicz, J., Waters, C. N., Summerhayes, C. P., Wolfe, A. P., Barnosky, A. D., Cearreta, A., Crutzen, P., Ellis, E., Fairchild, I. J., Gałuszka, A., Haff, P., Hajdas, I., Head, M. J., Ivar do Sul, J. A., Jeandel, C., Leinfelder, R., McNeill, J. R., Neal, C., Odada, E., Oreskes, N., Steffen, W., Syvitski, J., Vidas, D., Wagreich, M., and Williams, M.: The Working Group on the Anthropocene: Summary of evidence and interim recommendations, Anthropocene, 19, 55-60, 10.1016/j.ancene.2017.09.001, 2017.